A new approach to characterizing deposit type using mineral inclusion assemblages in gold particles

R.J. Chapman[1], J.K. Mortensen[2], M.M.Allan[3], R.D. Walshaw[1], J. Bond[4], K. MacWilliam[5]

[1] Ores and Mineralization Group, School of Earth and Environment, University of Leeds, Leeds LS29JT, United Kingdom

[2] MDN Geosciences Limited, Salt Spring Island, BC, Canada, V8K 1H4; and Department of Earth, Ocean and Atmospheric Sciences, University of British Columbia, Vancouver, BC, Canada, V6T 1Z4

*[3]Mineral Deposit Research Unit, University of British Columbia, 2020–2207 Main Mall, Vancouver, BC, Canada V6T 1Z4**

[4] Yukon Geological Survey, 2099 2nd Ave, Whitehorse, YT Y1A 1B5, Canada

[5]Newmont Mining Corporation, 166 Titanium Way, Whitehorse, YT Y1A 5P8, Canada

*Present address: Teck Resources Suite 3300, Bentall 5, 550 Burrard Street, Vancouver, B.C., Canada V6C0B3

Abstract

Mineral inclusions within native gold are features of lode gold occurrences that are preserved in detrital particles. Inclusion assemblages in populations of gold particles in placers from specific localities are revealed through inspection of polished sections, and assimilation of robust data sets permit reconstruction of the mineralogy of the lode source. Inclusion assemblages differ considerably according the source deposit type, and various approaches have been employed to graphically represent inclusion mineralogy. We present a simple method for depicting and comparing inclusion assemblages using a single standardized radar diagram template that illustrates the proportions of 11 metal and 5 non-metal (and metalloid) elements in each inclusion assemblage.

The Canadian Cordillera hosts many different gold-bearing deposit types, and is an ideal terrain in which to develop a globally applicable methodology. Although placer gold is widespread, the location and nature of source mineralization is commonly unclear. This study is based on the inclusion suites recorded in 37 sample sets of gold particles from both placer and lode localities. Radar diagrams describing inclusion assemblages show clear generic differences according to deposit type. Diagnostic signatures have been established and act as templates against which samples of unknown origin may be compared. This approach permits differentiation between populations of gold particles formed in different magmatic systems (low sulfidation epithermal, calc-alkalic porphyry, and alkalic porphyry) which may all be distinguished from gold formed in orogenic (amagmatic) mineralization. Metallic element signatures are most useful in differentiating gold from different magmatic-hydrothermal systems, whereas non-metallic elements allow for classification of orogenic gold sub-types.

Comparison of mineral inclusion signatures of gold in the Canadian Cordillera with samples from similar geologic settings worldwide suggest global applicability of this approach to gold fingerprinting. Therefore, the geochemical signature of inclusion assemblages provides a robust indication of the deposit type and may be applied in exploration to illuminate regional metallogeny in areas where relationships between placer deposits and their source(s) may be unclear.

Introduction

Orogenic belts host gold mineralization formed in both magmatic and metamorphic hydrothermal systems. Erosional products of mineralization include detrital particles of native gold, which may accumulate to form economic placer gold resources. The location of past and present placer mining activity can act as a vector in the exploration of bedrock deposits. Where detrital gold is present in smaller (subeconomic) concentrations, it may also provide valuable information to aid mineral exploration. Detrital gold is the best indicator for gold deposits (McClenaghan and Cabri, 2011), and a useful indicator mineral for Cu-Au porphyry deposits (Hashmi et al., 2015; Plouffe and Ferbey, 2017; Chapman et al., 2017, 2018); however, the simple presence of particulate gold in a panned concentrate is in itself not diagnostic of a specific deposit type. Consequently, indicator mineral methods have largely centred on other mineral species to help identify bedrock deposit types that are the source of the gold particles , including apatite (e.g., Bouzari et al. 2016; Mao et al., 2016), magnetite (e.g., Canil et al., 2016), and scheelite (Poulin et al, 2017, 2018). In common with all indicator mineral methodologies, the value of the approach is undermined if the target mineralization has already been removed by erosion.

This study focusses on gold mineralization within the Canadian Cordillera of British Columbia (BC) and Yukon. The study area comprises a complex collage of geological terranes that host auriferous orogenic, porphyry, epithermal, and reduced intrusion-related, deposits and we examine compositional variations in gold from all of these types of mineralization. Both Yukon and BC have been the focus of major exploration campaigns over the last several decades, which have resulted in the discovery of several potential deposits with gold as either as the primary commodity (e.g., orogenic gold at Coffee, Yukon), or as an important by-product (e.g., calc-alkalic porphyry Cu-Mo-Au deposit at Casino, Yukon; alkalic porphyry Cu-Au deposits at Mount Polley, Mount Milligan and New Afton in BC). The present study examines the generic relationships between inclusion suite mineralogy and deposit type, with the aim of developing templates by which detrital gold particles may be assigned to a specific origin. The advantages of successfully developing this methodology are threefold; i. it allows informed speculation on the geological setting of the source of economically important placer gold where this remains undiscovered; ii. it permits gold to be used as an indicator mineral during routine exploration; and iii. it permits characterization of undiscovered gold mineralization via placer occurrences, which can also inform regional metallogenic studies.

Geology and Metallogeny

The Canadian Cordillera in BC and Yukon is underlain by a complex assembly of pericratonic and oceanic lithotectonic terranes that were accreted to the Pacific margin of Laurentia in Mesozoic time (Fig. 1). These terranes are now separated from one another and from deformed rocks of the Laurentian margin by regional scale strike-slip and thrust faults. Gold-dominant or gold-bearing deposits occur throughout many of the accreted terranes in the Canadian Cordillera (Fig. 1), and locally within rocks of the deformed Laurentian margin. Gold-bearing deposits are particularly concentrated in the pericratonic Yukon-Tanana terrane in central and western Yukon and in adjacent basinal strata of the Laurentian margin (Fig. 1).

The Yukon-Tanana terrane (YTT) underlies a large region in southern and western Yukon, and extends southwards into northern BC and westwards into eastern Alaska (Fig. 1). The YTT comprises Devonian and older continental strata that form the basement to middle and Late Paleozoic magmatic arc assemblages. These units were deformed and metamorphosed multiple times, and subsequently intruded by five major syn- to post-collisional magmatic suites of Late Triassic to Paleogene age (Fig. 2). At least ten main metallogenic epochs have been identified in the region (Allan et al., 2013) ranging in age from Late Devonian to Paleogene, and representing a wide range of mineral deposit types that include orogenic gold, VMS, sedimentary exhalative, porphyry copper, skarn, and epithermal. From the perspective of significant gold mineralization, the most important metallogenic events include: (1) a flare-up of porphyry copper-gold and associated epithermal endowment in the Late Cretaceous (e.g., Casino, Sonora Gulch, Revenue, Klaza), (2) regionally widespread orogenic gold mineralization of Late Jurassic age in the Klondike and White Gold districts, and 3) fault-hosted, orogenic gold mineralization in the mid-Cretaceous (Coffee, Moosehorn Range). Allan et al. (2013) proposed that orogenic gold of the Sixtymile District (Figs. 1, 2) also formed part of the Jurassic metallogenic epoch on the basis of structural similarities.

A large number of gold deposits and occurrences are also present within and spatially closely associated with mid-Cretaceous felsic intrusions that were emplaced into deformed basinal rocks of the Laurentian margin (e.g., Dublin Gulch and Clear Creek; Fig. 2). These deposits are all considered to be examples of reduced intrusion-related gold deposits, and are part of the Tombstone Gold Province of Hart (2007).

Characteristics of natural gold that underpin mineralogical study

Gold alloy

Variations in the alloy composition of natural gold has long been recognised (e.g., Boyle, 1979). In some parts of the world, remuneration to placer miners is dependent on the purity of the gold collected, normally measured in 'fineness' (where fineness = (%Au x 1000/(%Au+%Ag)). Systematic recording of fineness of gold from various localities in placer camps globally showed that marked variation may occur between adjacent localities, which raised the possibility that specific placer gold deposits could be linked with a lode source by their alloy composition (e.g., Fisher, 1945). Initially this approach was possible only through consideration of bulk analyses of gold from either placer or lode environments, but rapid analysis facilitated by electron microprobe (EPMA) was ideally suited for characterizing whole populations of individual gold particles from a single locality. This approach permitted identification of the range of alloy compositions represented within a single population of particles from a single locality (henceforward 'sample population'), and also measurement of some other minor alloying elements such as Cu (e.g., Antweiler and Campbell, 1977) and Hg (e.g., Knight et al.,1999) where detectable. Several workers adopted an empirical approach to establishing placer-lode relationships through compositional characterization of sample populations using one of more components of natural gold alloy (Desborough et al., 1971; Craig et al., 1981; McTaggart and Knight, 1993; Loen, 1995; Knight et al., 1999). Morrison (1991) collated data from smelted gold from many important economic deposits worldwide to provide an overview of gold alloy compositional range according to deposit type, and subsequently Gammons and Williams-Jones (1995) described the chemical and physical controls on the Ag content of native gold and showed that changes in parameters such as pH, fS_2, and temperature may influence gold composition. These important contributions provided a platform to interpret the compositional range of gold populations in terms of their deposit type and ore forming processes (e.g., Townley et al., 2003; Chapman et al., 2009).

The degree of compositional variation between gold particles from a single locality may be pronounced (e.g., Chapman et al., 2010a) and hence a statistically valid population of particles is required to underpin mineralogical studies. The scarcity and value of gold has in some cases constrained the amount of material available to researchers, and for these reasons most early studies had a local focus, because the requisite sample size was only attainable in areas of active mining. In these situations, compositional variations of gold between localities permit the definition of different gold 'types' relevant to that area (e.g., Desborough et al., 1971; Antweiler and Campbell, 1977; Knight et al., 1999). The expansion of gold compositional studies to other areas was contingent upon the development of specific field methodologies which allowed the collection of sufficient gold particles in areas where overall abundance was low (Leake et al., 1997). This approach permitted regional studies of gold mineralization in areas of complex geology but with no current placer mining activity (Leake et al., 1998; Chapman et al., 2000a, b, c, 2005). Synthesis of outputs from different regional studies to generate larger datasets relating to gold formed in specific environments revealed overlap in the Ag content both with respect to geographical location within a single deposit type, and also between deposit types, which effectively precluded adoption of Ag content as a discriminant (summarised in Chapman et al., 2021). Nevertheless, comparison of the Ag range of sample populations at a local level remains an extremely useful approach to establishing their inter-relationship (e.g., Chapman et al. 2000b, Chapman and Mortensen, 2016) and extreme values of Ag (i.e., <1% or >35%) clearly indicate outlier conditions of formation.

The use of other minor alloying elements has made a larger contribution to our understanding of alloy composition variation between gold formed in different environments. Leake et al. (1991) identified a low Ag-Pd rich alloy formed in oxidizing low temperature chloride hydrothermal systems, in which gold particles were commonly associated with various intermetallic compounds of elements such as Au, Hg, Cu, Pd and Sb. Platinum group metals have also been associated with Cu-Au porphyry mineralization with high-K calc-alkalic or alkalic affinity (e.g., Tarkian and Stribny, 1999; LeFort et al., 2011), and this signature was recorded in gold alloy from various alkalic porphyry Cu-Au deposits in British Columbia by Chapman et al. (2017). The elevated Cu contents of gold from porphyry environments noted by Antweiler and Campbell (1977), Morrison (1991) and Townley et al. (2003) were also recorded by Chapman et al. (2018) in studies of auriferous calc-alkalic porphyry Cu-Mo-Au deposits in Yukon. Overall, gaining useful information of deposit type of gold solely from an alloy composition is dependent on the alloy compositions, and the majority of gold particles do not exhibit signatures diagnostic for deposit type when analysed by EPMA alone.

Laser ablation inductively coupled plasma mass spectrometry (LA-ICP-MS) permits identification of elemental components at the trace and ultra - trace levels, and several workers have applied the technique to compositional studies of gold (e.g., Watling et al., 1994,1998; Outridge et al., 1998; Crawford, 2007; Omang et al., 2015). The aim has been to measure a greater number of constituent elements in gold alloy, and hence generate further discriminants for deposit type. The development of methodologies which involved characterization of sample populations of gold particles according to Ag content using EPMA (e.g., Knight et al., 1999) had established that most gold particles exhibit a single Au-Ag ratio, and in those cases where alloy heterogeneity is observed, individual zones of different alloy composition also commonly appear homogenous when viewed in back scattered electron (BSE) mode. Consequently, it seemed reasonable to assume that minor and trace components of the alloy would also be present in uniform concentrations. Temporal analysis of plasma streams from ablated natural gold undertaken by Banks et al. (2018) revealed heterogeneity in element responses during excavation of the ablation pit. The authors speculated on whether small responses were a consequence of the partial ablation of inclusions or due to heterogeneous concentrations of elements within the gold alloy. Application of a time of flight (ToF) LA-ICP-MS system permitted Banks et al. (2018) to identify heterogeneity at all scales and concentration levels in many elements. The capability of the technique to establish spatial co-variance of elements lead to the identification of both small inclusions, whose elemental composition correlated with mineral species, and highly localised (typically c 1µm) elevations of other elements within the Au-Ag alloy. The degree of heterogeneity was such that different results could be obtained according to the positioning of the ablation pit (Chapman et al. 2021). It is clear that compositional studies of gold using LA-ICP-MS provides an advantage over EPMA studies because Cu and Hg are almostalways present and detectable. Nevertheless, the data available to date suggest that the original premise of gaining additional discriminants may not be valid, because individual elements are not present in every gold particle, and where present, their distribution may be highly heterogeneous. Consequently, there remains a need to analyse many particles to confidently characterize a sample population.

Mineral inclusions

Gold particles may contain inclusions of other minerals inherited from the lode source, as revealed in polished section (see typical examples in Figure 3). Our approach involves only inclusions completely encapsulated within gold particles and excludes any material adhering to the outside of the gold particle such as fragments of vein material or other mineral particles present owing to impaction. Inclusions related to the hypogene source mineralization were recognised at an early stage in compositional studies (e.g., Desborough et al., 1971). Whilst various other workers noted the presence of inclusions (e.g., Loen, 1995; Knight et al., 1999), the first systematic recording of inclusions within polished sections of gold particles was undertaken by the British Geological Survey (BGS) in studies within the United Kingdom (Leake et al., 1991,1992). Opaque inclusions such as sulfides, sulfarsenides and sulfosalts proved to be more useful than gangue minerals (typically silicates and oxides) for discriminating between different sample populations because they generally correlated with the unique mineralogy of the lode source (Chapman et al., 2000a). The abundance of opaque inclusions was shown to vary both between localities and depending on the amount of fluvial transport, in which particle deformation obliterates inclusions through exposure to the surficial environment (Loen, 1995; Melchiorre, 2019). The necessity of gaining a representative suite of inclusions for comparison between sample populations required development of specialized field techniques (Leake et al., 1997) to collect suitable numbers of gold particles. Correlation between inclusion speciation and alloy composition on a particle by particle basis generates a 'microchemical signature' and the synthesis of these two independent sources of information proved capable of distinguishing between gold from different sources at higher resolution than using alloy compositions alone (e.g., compare conclusions in Knight et al., 1999, and Chapman et al., 2010a). Nevertheless, the standard approach to regional studies has normally involved a primary characterization according to alloy compositions with inclusion suites providing additional information. This approach flowed from the belief that around 30 gold particles were required to generate a sufficient number of inclusions to characterize a sample population (Leake et al. 1997) but subsequent studies showed this number to be inadequate in areas where inclusion abundance is low.

The common association of placer gold deposits with orogenic gold districts also led to an initial bias in microchemical datasets to this deposit class. However, more recent studies focussed on magmatic-hydrothermal systems (e.g., Chapman et al., 2017, 2018) have shown that the concentration range of Ag in gold alloy is broadly equivalent to that in orogenic gold systems. Whilst in some cases the minor elements contributing to alloy compositions have proved diagnostic, their presence in individual particles is both sporadic and commonly near to their detection limit (LOD) using EPMA. Consequently, for the purposes of identifying generic signatures of natural gold according to source deposit class, the use of inclusion suites has provided a superior diagnostic criterion, and recent sampling campaigns have focussed on collecting sufficient particles to generate a robust inclusion signature.

This study focusses on inclusion suites recorded from a large number of sample populations throughout the Canadian Cordillera (Fig. 1). The range and complexity of the mineral inclusion suites has demanded development of a new approach to their interrogation, which we present below. The approach has been applied to inclusion suites from other localities worldwide to evaluate the degree to which signatures that are diagnostic for deposit class within the Canadian Cordillera are globally applicable.

Origin of inclusions

Although inclusions have been recorded in many of the studies described above, discussion has centred on their composition and abundance rather than considering fundamental controls on their formation. Chapman et al. (2000a) showed a close correlation between inclusion suites and vein mineralogy of proximal auriferous mineralization at some localities in the UK and Irish Caledonides, and similar relationships have been recorded in the Canadian Cordillera (e.g., Fig. 3A) in both orogenic (e.g., Chapman and Mortensen, 2016) and magmatic-hydrothermal (Chapman et al. 2017, 2018) settings. The majority of inclusion minerals such as pyrite, arsenopyrite, chalcopyrite, sphalerite, and galena are clearly manifestations of common vein minerals (Figs. 3B-E).

Tiny inclusions of minerals within a different host are a common feature in many deposit types. Well known examples include blebs of PGM at the margins of sulfide mineral grains (ascribed to nucleation and growth at mineral boundaries: Godel et al., 2015), and gold inclusions in Cu-bearing sulfides in porphyry systems (ascribed to exsolution of Au from a recrystallizing sulfide intermediate solid solution: Simon et al. 2000). In gold particles, inclusion formation by exsolution is not a plausible general mechanism because of the relative size of inclusions and their gold host (e.g., Fig. 3D). Coeval precipitation with Au is favoured as this clearly correlates with the inclusion-ore assemblage relationship. In some cases, the process of formation of gold particles may be incompatible with inclusions. Gold growth on sulfides induced by electrochemical processes was described by Moeller and Kirsten (1994). Here, deposition of gold alloy is induced electrochemically, initially onto pyrite and subsequently facilitated by the conductivity of the precipitated metal. Petrella et al. (2020) described the aggregation of gold nanoparticles expelled from silica gel during quartz crystallization to form visible particles. Neither of these processes would be expected to generate gold particles containing inclusion species common to the host mineralization. Consequently, sample populations in which inclusions are absent may also inform the mechanisms of particle formation.

The presence of rare minerals as inclusions may also be a consequence of co-precipitation with Au, but there is another explanation in those cases where the inclusions are extremely small (<1µm). Banks et al. (2018) employed LA-ICP-MS on polished sections of gold particles and showed that they were commonly heterogeneous at a sub - micron level. The presence of elements otherwise unrecorded in the host mineralogy (e.g., Pt, Pd or Bi) raises the possibility of incorporation of nano particles formed prior to the onset of gold precipitation. The formation of these particles could be divorced from the environment of hydrothermal gold, but they may be scavenged during growth of the gold particles. Very tiny inclusions of rare minerals could represent the large end members of this process, but irrespective of the mechanism of their formation, they provide an insight into the fluid chemistry of a specific hydrothermal system.

In summary, the suite of inclusions observed within populations of gold particles are indicators of the ore mineral assemblage. Whilst further work is required to clarify the processes by which all inclusions are formed, their mineralogy is intrinsically linked to the process of mineralization.

According to the principles discussed above it would be expected that the mineralogy of inclusion suites varies according to the widely ranging source-transport-trap pathways operating in different mineral deposit types. The inclusion assemblage in gold from magmatic-hydrothermal systems would be constrained by the geochemical signature of the intrusion type, the resulting ore fluids and the relative importance of chloride and hydrosulfide ligands at any point in the evolving system. Fluid-rock interaction pathways are typically short, and often wholly contained within juvenile igneous rocks of the intrusion. Thus, the inclusion suite within gold is related only to the elemental signature of the magmatic fluid. The mineralogy of orogenic gold deposits differs from that observed in magmatic hydrothermal systems as a consequence of the ore fluid which is normally circum-neutral, CO_2-rich, and relatively low in $Cl^{-}_{(aq)}$. Ore fluids may follow an extended pathway facilitating interaction with a wide variety of lithologies and associated fluid modification, according to specific setting (Liu et al. 2021).

Methodology

Sample collation and analysis

Data for this study are drawn both from new and existing datasets of gold from both lode and placer settings in the Canadian Cordillera (Table 1a-b), together with data derived from other studies worldwide (details in Table 1c). Details of individual sample localities, used to generate the data sets described in Table 1 are provided in the Supplementary material. Localities of samples from the Canadian Cordillera are shown on a simplified tectonostratigraphic terrane map in Figure 1. In some cases, individual sample populations from the same or adjacent drainages have been combined where there is evidence for compositional uniformity based on alloy analysis. In cases where single drainages yield compositionally distinct sample populations that reflect multiple bedrock sources, the samples are presented separately (e.g., Henderson Creek, Yukon). Details are provided in Table 1. Inclusions have been identified by manual visual screening of polished sections using an SEM both in BSE and secondary electron (SE) modes. Analytical details are provided in the relevant citations.

Previous methods used to depict inclusion suites.

There are several challenges to depicting inclusion suites such that their inter relationships are clear. Tabulated data and histograms were quickly replaced by ternary and spider plots (e.g., Leake et al. 1997; Chapman et al. 2000a, Chapman et al., 2017; Moles and Chapman, 2019), but each exhibits drawbacks when comparing a number of data sets which differ according to the inclusion species present. Figure 4 provides various approaches to depicting sample sets of gold from orogenic, orogenic epizonal (see later discussion), low-intermediate sulfidation epithermal, calk-alkalic porphyry Cu-Au-Mo and alkalic Cu-Au porphyry mineralization. Silver contents of the various populations are also included, as many previous studies focussed on the use of Au-Ag ratios as a discriminant. Figure 4A shows that that whilst a greater proportion of gold particles from the epithermal locality and calk-alkalic porphyry locality exhibit relatively high and low Ag ranges respectively, there remains a considerable overlap in Ag range between sample sets, such that the Ag content of an individual particle is not diagnostic of deposit type. Triangular diagrams have previously been employed to depict inclusion suites in various studies with a regional or deposit type focus, and in these cases the range of inclusion species encountered is limited. Such diagrams become difficult to interpret when a wide range of metallic elements are present in the various inclusion assemblages, but even so, in Figure 4B, the inclusion data set is not fully represented. Consequently, a generically applicable graphical template to depict inclusions assemblages cannot be based on triangular diagrams. The issue of complex inclusion assemblages or variation between inclusion assemblages may be partially alleviated by the use of spider diagrams. Figure 4C provides a spider plot for the five sample sets featured in the triangular plots in Figure 4B. Organization of the horizontal axis groups minerals which share chemical similarities, and groups which are commonly associated in important deposit types are placed adjacently, such that characteristic plot shapes are generated. For example, gold from orogenic hydrothermal systems is commonly defined by an inclusion suite containing base metal sulfides, whose presence is more easily viewed by clustering of pyrite, galena, chalcopyrite and sphalerite on the x-axis.

The main limitation to this approach is that a maximum of four or five plots may be compared before the figure becomes illegible. In addition, many minerals present as inclusions within gold from magmatic-hydrothermal systems show substitution of elements into a mineral lattice (e.g., Bi or Sb in PbS; Chapman et al., 2018). It is important to make a distinction between relatively pure galena (a common inclusion mineral in gold from orogenic systems) and galena containing Sb or Bi which is most commonly associated with a different origin. Accommodation of degrees of substitution in a spider diagram would result in an extended horizontal axis in which it would be impossible to place related minerals adjacently, because of the range of substitutions involving several elements.

Development of a new approach to represent inclusion suites.

Studies of both orogenic and magmatic-hydrothermal systems has shown that characterization of inclusion suites may point to a diagnostic elemental association; e.g., the Bi-Pb-Te-S association in gold particles from calc-alkalic porphyries. Characterization by elements takes into account both the variable mineralogy and solid solutions within minerals that may be locally significant. An empirical approach to semi-quantitative characterization of an inclusion assemblage has been developed which permits simultaneous evaluation of the relative importance of metallic and non-metallic elemental components using radar diagrams. Consideration of the inclusion suites recorded in all studies to date resulted in the selection of the following metals for consideration: Fe, Cu, Pb, Zn, Ag, Bi, Mo, Hg, Pd, Ni and ‘other’. Non-metals and metalloids comprise: S, As, Sb, Se, and Te. The arrangement of the axes places elements which commonly co-exist adjacent to one another, because the resulting “radar plot” generates two dimensional shapes which afford easier visual comparison than a number of radiating lines.

Radar diagrams have been generated through adoption of a scoring system for each inclusion species recorded in a single particle cross-section. In this study we include only ‘ore minerals’ (i.e., sulfides, sulfarsenides, sulfosalts, selenides and tellurides), as these have proved far more diagnostic than gangue minerals. Nevertheless, atypical abundances of minerals such as barite, monazite and xenotime may prove informative in some cases. Individual inclusions are scored in terms of their metallic and non-metallic/metalloid chemical components. The total score for metals within each inclusion is 1, and the same total applies to non - metal components. The stages involved in scoring a sample population and the justification for scoring criteria and figure design are described in Table 2. A schematic diagram which describes the entire inclusion recording and characterization process is provided in Figure 5.

The diagrams which underpin this paper comprise ‘tiles’ of metal and non-metal plots for each locality. Tiles on the top rows of Figures 6 and 7 are those where the provenance of the sample population is clear, either because the sample is derived from ore, or because the placer-lode relationship is uncontentious. Lower rows include sample populations from placer localities where the location of the source is unclear, placed directly underneath similar signatures of gold of known provenance. Lode and placer samples have been differentiated by use of heading style on each tile.

Figure 4D shows five pairs of radar diagrams depicting the inclusion assemblages of the samples previously illustrated by spider and triangular plots. The resulting plots permit rapid evaluation of the key elements in each signature and a convenient way to compare multivariate data simply by comparing the shape of the 2D plot. The entire inclusion assemblage is represented, and the provision of an 'other' category enables flexibility for acknowledging the presence of rarer elements when they occur. In particular the approach makes clear differences in the proportions of non-metallic components in a far superior fashion to S-As-Te triangular diagrams which have found use elsewhere.

Characterization of inclusion signatures

Main distinguishing characteristics of gold from orogenic and magmatic hydrothermal systems

Inclusion suites of gold from orogenic settings are typified by a non-metal signature dominated by sulfides usually exhibiting contributions from As±Sb±Te. Iron provides the dominant metal contribution with other elements largely confined to base metals and in some cases Ag. In contrast, gold formed in magmatic hydrothermal environments exhibits a far greater variety of metal elements. In general, non- metallic elements provide a means to characterizing orogenic gold from different localities, whilst metal signatures are more useful for defining signatures of gold from magmatic hydrothermal systems. More detailed consideration of the elemental signature of inclusion assemblages revealed in radar diagrams relating to gold from many different localities is provided below.

Orogenic gold systems

The inclusion signatures of orogenic gold systems are presented in Figures 6 and 7 where the diagrams have been arranged to show transitions from S- (S+As+Sb) and S-(S+Te) respectively. The (S+As+Sb) signature has been recorded throughout the study area, whereas the (S-Te) signature (always accompanied by Ag) is confined to various occurrences throughout central Yukon. The spatial relationship of localities where gold exhibits the (S+As+Sb) and S-(S+Te) signatures is not zoned, and individual examples of each may be less than 10 km apart (e.g., the Boulder Lode and Nugget samples (Fig. 6) are within a few km of localities which generated Lone Star types 1d and 1f (Fig. 7). Coincidence of As and Te is limited to sample populations from Thistle Creek and Henderson Creek. Other outlying signatures are observed in gold from Henderson Creek (complex metal signature and Scroggie Creek (strong Te signature).

Magmatic-hydrothermal systems

Figure 8 compares inclusion signatures of gold from various magmatic-hydrothermal systems. A previous study by Chapman et al. (2018) characterised signatures from gold derived from calc-alkalic porphyries and associated epithermal systems and identified a generic Bi-Pb-Te-S signature which is clearly visible in the radar diagrams describing gold from Casino and Nucleus-Revenue. New data describing placer gold from the drainage surrounding the KSM porphyry deposit in northwestern BC (Fig. 1) also shows this association. Other Yukon calc-alkalic porphyry prospects at Sonora Gulch and Cyprus yielded inclusion suites compatible with this proposed generic signature, but insufficient inclusions were observed to generate a radar diagram. Porphyry-epithermal transitions at Casino are linked to a reduction in the Cu abundance in the inclusion suite, and an increase in As, whereas Bi and Te persisted (Chapman et al. 2018). Gold inclusion suites from the epithermal localities exhibit a clear Ag-Pb signature, and the Blackdome locality also returned a very strong Se signature. Gold inclusion suites from alkalic Cu-Au porphyry systems exhibit a diagnostic Pd-Hg signature, as described by Chapman et al., (2017). These elements also contribute to the alloy signature in some particles and the Pd-Hg association is a diagnostic marker for gold of this type.

New data describing the inclusion suites from reduced intrusion-related gold systems reveal elemental signatures consistent with mineralogical associations previously reported. The inclusion suite of placer gold from Dublin Gulch exhibits a Au-As- Pb-Mo-Bi association which is a composite of mineralogical associations in three auriferous stages reported by Cave et al. (2019). Placer gold from Clear Creek on the periphery of an intrusion related system in the Tombstone belt west of the Eagle deposit (Fig. 2) generated a Pb-As-S signature in the inclusion suite.

The relatively small amount of data available to this study describing inclusion suites in gold from low and intermediate sulfidation epithermal systems suggests that signatures are variable and complex. The inclusion signatures of gold from Klaza and Canadian Creek (Fig. 2), share a strong Ag-Te signature, whereas a Se signature is recorded in lode gold particles from Blackdome in south-central BC (Fig. 1). The Stirrup Creek placer locality is downstream of the Astonisher low sulfidation epithermal Au-Ag occurrence (Flower, 2018; Fig. 1). The inclusion signature shows dominant Te, but Ag is apparently absent.

The Wheaton Creek placer in northeastern BC (Fig. 1) is underlain by ultramafic lithologies. Many gold particles show marked exsolution textures of tetra auricupride in a Au-Ag-Cu matrix (Knight and Leitch, 2001). The inclusion suite comprises predominantly Cu-bearing sulfides, showing varying Fe concentrations, which generate a distinctive radar plot (Fig 8).

Discussion

Overview of signatures of gold from orogenic and magmatic-hydrothermal systems

Sample populations from BC and Yukon show that inclusion suites from orogenic gold systems shows a simpler elemental signature (S±As±Sb±Te and Fe±Cu±Pb±Zn) than gold from magmatic-hydrothermal systems. Tellurium is also an important component of the element suite in gold from magmatic-hydrothermal systems, but the Te mineralogy is more complex than in gold from orogenic systems where it is usually confined to minerals in the Ag-Au-Te-S system. Gold formed in magmatic-hydrothermal systems generally exhibits more complex elemental signatures, likely reflecting both the nature of the ore fluids and the wider range of possible physicochemical conditions under which gold may precipitate (Chapman et al., 2017, 2018). Both oxidized calc-alkalic porphyry and reduced intrusion-related systems are present in Yukon, but gold formed in each deposit type may be distinguished according to the inclusion assemblage. The Eagle intrusion - related Au deposit of the Tombstone gold belt (Fig. 1A) comprises three auriferous vein stages; the 'Eagle Style', and 'Potato Hills Styles 1 and 2' (Maloof et al. 2001; Cave et al. 2019). Gold containing inclusions of molybdenite corresponds to the Eagle Style whereas galena and Pb-Bi sulphides occur in all styles. The relatively high abundance of arsenopyrite inclusions suggests a stronger Au-As link than indicated in the paragenetic associations presented by Cave et al. (2019). Whilst Bi –bearing minerals are present, they are far less common than in gold from calc-alkalic porphyry systems. Additionally, arsenopyrite is a major component of the inclusion suite in gold from Dublin Gulch, but is largely absent in gold from the porphyry systems in the region (Chapman et al. 2018). The auriferous sheeted quartz veins in the Clear Creek drainage (Marsh et al., 2003) are the source of placer deposits, where the inclusion suite is dominated by the major associated minerals pyrite, pyrrhotite and arsenopyrite.

Whilst the dataset describing epithermal systems is relatively small, the general geochemical evolution of porphyry to low/intermediate sulfidation epithermal systems is reflected in decreased Cu and increased Ag, Pb and Zn within the inclusion signatures. Bismuth and tellurium signatures are present in epithermal as well as calc-alkaline porphyry-related gold, and these coupled with a complex metal signature provide a means to distinguish epithermal gold from that formed in most orogenic gold systems. The low sulfidation epithermal gold sample from Blackdome also exhibits a strong Se signature from naumanite (Ag_2Se), and Se was also recorded in a Bi-Te – bearing inclusion in a gold particle from Sulphurettes Creek, at KSM (Fig 1).

Implications of inclusion signatures for deducing regional gold metallogeny

Most sample suites from BC described in this study originate from areas where the deposit type is known. Gold derived from orogenic mineralization in BC (Bralorne, Cassiar, and the Cariboo Gold District) shows signatures very similar to many observed in gold from Yukon localities. Other sample suites from Atlin and the Cow Mountain area in the Wells-Barkerville camp, BC, deviate in metal signatures and are discussed below.

In contrast, the location and deposit type of lode sources of gold for many economically important placers in Yukon is unclear, mostly because of extremely poor bedrock exposure. Nevertheless, numerous exploration campaigns have been based on the presence of locally abundant detrital gold in streams, but in areas where both metasedimentary sequences and igneous intrusions occur, target identification may be handicapped by different potential sources. If multiple lode source types are indeed present, they may be identified and their relative importance deduced from consideration of the inclusion suites observed within detrital gold. For example, inclusion assemblages from both the Sixtymile District, the Last Chance Creek area of the Klondike District and Tenmile Creek area (Fig. 2) show the S-As signature and a metal suite dominated by Fe, plus various base metals (Fig. 6). In each case, the gold inventory of placer deposits is mostly of orogenic origin, and if present, gold derived from auriferous mineralization associated with local intrusions is subordinate. The sample population from the Indian River area (Fig. 2) also exhibits the S-As signature but probably contains gold particles from both local and distal origins (Chapman et al., 2011), which may explain the slightly more complex metal radar plot.

Some sample populations of the S-As signature type also exhibit a small contribution from sulfosalts. This signature is evident in gold from Bralorne, Cassiar and the Siwash Creek placer. In other cases, the Sb signature is pronounced and clearly associated with Pb and As; e.g., gold from drainages near the epizonal orogenic Coffee gold deposits (Fig. 2). This signature is very similar to the Sb-Pb-As signature of gold from the Moosehorn Range on the southern Yukon-Alaskan border. Allan et al. (2013) characterised both systems as Cretaceous orogenic systems distinct from the earlier Jurassic examples elsewhere in west-central Yukon. Whilst the particle size of gold from the Cretaceous orogenic Coffee deposit is too small to accumulate to any significant degree in placer deposits, the ore shows a strong Au-As-Sb association (Wainright et al., 2010; MacWilliam, 2018). Consequently, there is strong evidence to link an unusual signature to a specific orogenic setting in the western Dawson Range, implying generic influences on ore fluid composition.

Gold from veins at Mackinnon Creek, in the White Gold district, Yukon, shows a distinctive Ag-Te signature (Fig. 7) largely due to the presence of hessite, and this association is replicated in several sample populations of placer gold from west-central Yukon. The presence of Te is commonly associated with magmatic-hydrothermal systems (e.g., Baker et al. 2005) but the mineralization at Mackinnon Creek has been dated at 157.3±2 Ma, within a significant gap in regional magmatism (Allan et al., 2013). These authors also describe a period of regional uplift and several instances of mineralization and textures within several different orogenic systems indicative of formation at relatively shallow depths. Correlation of gold mineralization at Mackinnon Creek with that derived from regional placer deposits show commonality both in terms of the radar diagrams and other accessory minerals (e.g., abundant barite inclusions in gold from Thistle Creek). Chapman and Mortensen (2007) suggested that the mineralogy of placer gold from Eureka Creek (Yukon) and environs (illustrated in Fig. 7) was indicative of epithermal mineralization; however, Wrighton (2014) argued that an epizonal orogenic gold source was more likely based on, i: a nearly identical signature to one gold type (1d) from the Lone Star deposit, Klondike, Yukon (Chapman et al., 2010); and ii. the replication of this signature at several other placer and lode localities with no clear igneous affinity. The similar P-T-X conditions of both epizonal orogenic gold and magmatic-related epithermal mineralization would be reflected in mineral assemblages paragenetically related to gold; for example, the clear Au-adularia association in Eureka Creek (Chapman and Mortensen, 2007). Here we propose that the Ag-Te signature reflects a late stage episode of mineralization within the Late Jurassic orogenic gold event, whose widespread nature may be related to the diachronous uplift in the region described by Staples et al. (2016).

The Ag-Te signature has been observed in placer gold from Eureka Creek, Adams Creek (Lone Star area), Thistle Creek and environs, Maisy May Creek, and Scroggie Creek, all in west-central Yukon (Fig. 2). With the exception of sample sets from Henderson and Maisy May creeks (Fig. 2), the Ag-Te signature is associated with elevated Hg in the alloy or presence of Hg minerals in the inclusion suite. In most cases Te and As are mutually exclusive, but exceptions are gold from Thistle Creek (which is otherwise similar to the others), and Henderson Creek and tributaries, which exhibit a far more complex signature (Fig. 7). Currently it is unclear whether the mixed As-Te signature results from mixing of gold particles from different sources in the same drainage. Overprinting of pre-existing Cu and Mo-bearing mineralization at Lucky Joe and Rebecca (Henderson Creek catchment) was described by Allan et al. (2013) and may also have occurred in the main Henderson Creek drainage. If so, additional input from as yet undefined sources may be plausible explanation for the presence of Bi and Mo in placer gold samples from North Henderson Creek, and the elemental complexity of the inclusion signature from the middle reaches of Henderson Creek. There are sufficient similarities between the gold samples from Henderson Creek and other regional Ag-Te signatures to suggest a genetic relationship, but influences of specific local lithologies could account for other geochemical variation, which may extend to the absence of Hg in the Au alloy. Gold from Scroggie Creek exhibits a very strong Te signature generated by the presence of altaite and melonite inclusions in addition to hessite. These minerals indicate higher *f*Te than present elsewhere (Affifi et al., 1988), and Allan et al. (2013) note an unusually high degrees of potassic alteration at this locality.

The sample suites from the Atlin placer camp in northern BC and the Cow Mountain area in the Wells-Barkerville area (Fig. 1) deviate from all other samples because of the presence of Ni and Ni+Bi respectively (Fig.6). Nickel-bearing inclusions are regularly encountered in gold compositional studies and we hypothesize that their abundance could be influenced by fluid interaction with local host lithologies, such as ultramafic rocks or black shales which contain elevated Ni levels. The high incidence of Bi at Cow Mountain is a consequence of the mineral cosalite ($Pb_2Bi_2S_5$) but the Bi-Te association, characteristic of gold from magmatic-hydrothermal systems (e.g., Chapman et al., 2018), is absent. The reasons for the uniquely strong Bi signature in this orogenic setting remain unclear. There may be a relationship to the '5 element' Ag-Ni-Co-As +/- Bi-U veins of BC (Lefebure, 1996) in which Ni-Co-Fe arsenides, Ni-Co-Fe-Sb sulfarenides and Bi minerals are common.

Potential for inclusion signatures as generic indicators of source deposit type

Comparison of inclusion suites of samples from the northern Cordillera with others from similar geological environments globally is constrained by the availability of sample sets. The northern Cordilleran sample sets are relatively large and were collected with a view to generating suitably large inclusion suites whereas those from previous campaigns elsewhere were sufficient to characterize alloy variation, but in many cases the inclusion count was small. In addition, only recent studies of detrital gold in West Africa (Dongmo et al., 2019; Fuanya et al., 2019) and Russia (Lalomov et al., 2016; Zaykov et al., 2017; Svetlitskaya et al., 2018; Nevolko et al., 2019) have systematically studied large gold grain populations and their inclusion assemblages. Gold from Precambrian granite-greenstone terranes in northern and central Africa show very low inclusion abundances and generation of radar diagrams has not been possible (Ngomo et al., 2019; Fuanya et al., 2019; Chapman et al. 2021) . Published data describing gold signatures from economically significant Russian placers has focused on samples from trunk drainages which commonly contain gold from several different sources of mineralization, which again precludes generation of radar diagrams specific to a single deposit type. Nevertheless it has been possible to generate some useful datasets describing orogenic gold from Phanerozoic mineralization in the UK Caledonides (data from Leake et al., 1998; Chapman et al., 2000; Moles and Chapman, 2019) and Malaysia (Henney et al., 1994). Figure 8 compares signatures of these sample populations with some typical signatures of orogenic Cordilleran gold. The S-As-base metal signature, typified by the sample population from Last Chance Creek, Yukon, was recorded in gold from both Leadhills (southern Scotland) and Lubuk Mandi, Malaysia, where gold mineralization is hosted in metasedimentary rocks. The 'Bralorne type' signature (S-As-Sb- base metal) was observed in gold from localities in the central southern Uplands of Scotland and Co. Wexford, Ireland. A more complex non-metal signature of S-As-Sb-Te coupled with a pronounced Ni signal characterizes gold populations from the Atlin placer camp, BC, and the Mayo subterrane, Ireland. In both localities, gold mineralization is hosted in a mixture of metasedimentary and ultrabasic lithologies. In general the S-As-Sb association appears more common than the S-Te association.

Gold from two epithermal districts is available for comparison with northern Cordilleran samples (Fig. 9). Chapman et al. (2005) identified two main signatures in placer gold hosted by Devonian high K calc-alkaline volcanic rocks in the Ochil Hills, Scotland and confidently ascribed an epithermal origin to both. Type 1 gold occurred throughout the region (Table 1) and comprises contributions from several metallic elements and a S-As-Te non-metallic signature, which is most similar to that recorded at KSM, a calc-alkalic Cu-Au deposit. Type 2 gold was further characterized by Chapman and Mortensen (2007) according to two phases of mineralization: a low-Ag type with an inclusion signature dominated by Bi telluride and a high-Ag alloy, commonly replacing the primary low-Ag alloy in individual particles, which hosted an inclusion suite containing wittichinite (Cu_3BiS_3) and hessite. The elemental signature of the inclusion suites of the two sub-types differs mainly in the presence of Ag in the second phase which is consistent with elevated Ag in the host alloy. The absence of As in the signatures most closely corresponds with the signature of gold from the Casino Cu-Au-Mo-Ag porphyry deposit in Yukon (Fig. 8). A dominant Te signature is also evident in the epithermal mineralization associated with alkalic volcanic rocks from the Wainmanu River in Fiji (Fig. 9) (Naden and Henney, 1995). Overall, the epithermal gold signatures are considerably more complex than those from orogenic settings, with a Te-signature (usually pronounced) and varying contributions from As and Te, as well as Se in the case of Blackdome in BC.

Implications for use of gold as an indicator mineral

Historically the potential for inclusion suites to provide evidence of gold particle provenance has been undervalued. Researchers have preferred to characterize sample populations based on alloy compositions, an approach requiring fewer particles to produce statistically valid results, but only yielding diagnostic features useful outside geographically focussed studies if Ag concentrations are extreme, or if additional alloying metals are detectable. In the present comparative study, radar diagrams are used as an effective method of depiction and comparison of gold populations, but with some limitations. Firstly, sufficient large populations of analysed inclusions are required to generate a meaningful plot. The number of inclusion records required to generate robust data increases with mineralogical complexity. Mineralogically simple inclusion suites such as those generated from many sample populations of gold from orogenic mineralization may be yield useful diagrams with around ten data points but the complex signatures observed in gold from many magmatic-hydrothermal systems require larger datasets in order to represent the wider range of metals present in inclusion minerals. The radar plots themselves provide a semi quantitative approach to defining elemental compositions within a sample set, with the simultaneous depiction of 16 variables providing a robust basis for classification. In general, indicator studies involve comparison of data sets from an unknown with that of a template. In the case of the methodology developed in the present study, small inclusion suites of around 10 data points can be ascribed as compatible or incompatible with a compositional template, and such judgements do not demand quantitative parity. For more complex inclusion assemblages a minimum of 15 inclusions appears advisable (Chapman et al., 2021). In some cases, deviations from a ‘standard’ signature can be informative. For example, the enhanced Ag and Te signature observed in gold from several orogenic settings represents the addition of hessite (Ag_2Te) to the more commonly encountered orogenic inclusion assemblage. Results such as this provide an insight into specific conditions of ore formation rather than representing an issue with a more widely applicable template.

Enhancing the quantity of data from an individual sample population through multiple sectioning could alleviate issues surrounding small populations of inclusions. We have not adopted this approach because of its destructive nature, that would preclude future application of other analytical techniques to previously characterised samples. Examples are provided by recent studies using time-of-flight laser ablation systems to generate trace element maps and correlation of these data sets with crystallographic studies undertaken using EBSD (Chapman et al., 2021). Secondly, mineralogical information is lost in translation to element data and this may be important where mineral species might themselves be diagnostic markers. Both these drawbacks can be mitigated in the design of workflows.

The present study has utilized specialist field skills to collect the requisite number of particles, but similar sized populations can also be obtained from placer mining operations, either through donation or purchase. Whilst the abundance of inclusions in particle sections varies between sample populations from different localities and deposit types, consideration of published data (summarised in Chapman et al., 2021) shows a typical range of 5-15%. Consequently, between 150 and 250 particles should yield a useful inclusion suite. Subsequent analysis of the alloy compositions either by EPMA or LA-ICP-MS need not necessarily involve all particles, as long as those with inclusions are characterized. Mineralogical data are scrutinized during the production of radar diagrams and significant mineral associations or individual mineral species may be identified at this stage and interpretations influenced accordingly.

We advocate a change in approach to gold compositional studies which uses inclusion data as the primary criteria, supported by considerations of alloy composition. This approach provides far more information than the current standard approach of initial focus on characterizing alloy concentration profiles with the consideration of inclusion suites if fortuitously sufficiently large.

The approach described here also has the potential to be combined with standard methodologies of stream sediment sampling, both in relation to the fines fraction and heavy mineral concentrates. Moles and Chapman (2019) undertook a case study of the Caledonides of SE Ireland in which all three methodologies were applied. These authors proposed a stage wise approach in which standard sediment fines analysis provided a rationale for the more labour-intensive targeted gold collection stage. Consideration of heavy mineral concentrates provided valuable information on surface sediment mobility in glaciated areas and would doubtless illuminate the potential for different deposit types in regions such as the North American Cordillera, but such samples rarely contain sufficient gold particles for characterization. The inclusion suites of gold particles provided by far the best indication of the nature of local gold mineralogy, and we advocate their description through adoption of the radar diagram approach in future integrated studies.

Conclusions

1. Analysis of gold inclusion signatures is a superior approach to establishing the source deposit type than simply considering the composition of Au-alloy since it yields information about ore mineral assemblages and element associations.
2. The use of radar diagrams to show proportions of different elements provides a convenient method to compare signatures of different populations. Nevertheless, consideration of specific inclusion species and in some cases Au alloy compositions may contribute to the overall interpretation.
3. Inclusion signatures can differentiate between gold formed in magmatic-hydrothermal and orogenic gold (amagmatic) systems.
4. Orogenic gold mineralization is best characterized according to the non-metallic S±As±Sb signature, and in most cases metallic elements are restricted to Fe, Cu, Pb and Zn
5. The range of orogenic gold signatures is a function of divergent fluid compositions arising from the wide range of fluid-rock interactions afforded by extended fluid pathways.
6. The S-Te-Ag signature present in gold from many localities in Yukon is associated with an epizonal sub-type of orogenic gold with mineralogy showing similarities to that formed in some epithermal environments.
7. Gold formed in alkalic and calc-alkalic porphyry settings may be distinguished by their Pd-Hg and Bi-Pb-Te-S signatures, respectively.
8. Whilst a limited number of epithermal localities was available to the study, the range of inclusions signatures are distinct from those observed in gold form either orogenic or porphyry systems. Tellurium is ubiquitous and Bi is normally present together with a wider range of metals than is associated with orogenic gold. Most sample populations exhibit a strong Ag signature in common with gold from epizonal orogenic environments.
9. In lithologically complex areas with the potential for multiples types of gold mineralization, explorationists can employ inclusion suites to establish the regional extent of a particular type of gold mineralization. Thus exploration strategies can be informed by both presence of placer gold and an understanding of the source type.
10. An initial comparison of inclusion templates describing gold from the Canadian Cordillera with other examples globally suggests that inclusion signatures are generic to style of mineralization and geological setting.

Acknowledgements

We are indebted to Dr Beth McClenaghan and Dr John Youngson for their thorough, constructive and generally helpful reviews that greatly improved this manuscript. We also thank the Department of Earth and Ocean Sciences at the University of British Columbia for access to sample collections originally assembled by John Knight. Further analyses of samples from these collections was facilitated by funding received from Geoscience BC as part of the 'Gold Atlas for British Columbia' project.

References

Affifi, A.M., Kelly, W.C., and Essine, E.J., 1988, Phase relations in the tellurides, sulfides and oxides: applications to telluride-bearing ore deposits: Economic Geology, v. 83, p. 395-404.

Allan, M. M., Mortensen, J. K., Hart, C. J. R., Bailey, L., Sanchez, M. G., Ciolkiewicz, W., and Creaser, R. A., 2013, Magmatic and metallogenic framework of west-central Yukon and eastern Alaska: Society of Economic Geology, Special Publication no. 17, p. 111-168.

Antweiler, J.C. and Campbell, W.L., 1977, Application of gold compositional analyses to mineral exploration in the United States: Journal of Exploration Geochemistry, v. 8, p. 17-29.

Baker, T., Pollard, P.J., Mustard, R., Mark, G., and Graham, J.L., 2005, A comparison of granite-related tin, tungsten, and gold-bismuth deposits: Implications for exploration: Society of Economic Geologists Newsletter, no. 61, p. 5–17.

Banks, D.A., Chapman, R.J. and Spence-Jones, C.P., 2018, Detrital gold as a deposit-specific indicator mineral by LAICP-MS analysis: Geoscience BC Report 2018-21, http://www.geosciencebc.com/s/2016-006.asp

Bouzari, F., Hart, C.J., Bissig, T. and Barker, S., 2016, Hydrothermal alteration revealed by apatite luminescence and chemistry: a potential indicator mineral for exploring covered porphyry copper deposits: Economic Geology, v. 111, p. 1397-1410.

Boyle, R.W., 1979, The geochemistry of gold and its deposits: Geological Survey of Canada Bulletin, 280 p.

Canil, D., Grondahl, C., Lacourse, T. and Pisiak, L.K., 2016, Trace elements in magnetite from porphyry Cu–Mo–Au deposits in British Columbia, Canada: Ore Geology Reviews, v. 72, p. 1116-1128.

Cave, B.J., Barnes, S.-J., Pitcairn, I.K., Sack, P.J., Kuikkad, H., Johnson, S.C. and Duran, C.J., 2019, Multi-stage precipitation and redistribution of gold, and its collection by lead-bismuth and lead immiscible liquids in a reduced-intrusion related gold system (RIRGS); Dublin Gulch, western Canada: Ore Geology Reviews, v. 106, p. 28-55.

Chapman, R.J., and Mortensen, J.K., 2007, Application of microchemical characterization of placer gold grains to exploration for epithermal gold mineralization in regions of poor exposure: Journal of Geochemical Exploration, v. 91, p. 1–26.

Chapman, R.J., and Mortensen, J.K., 2016, Characterization of gold mineralization in the Northern Cariboo gold district, British Columbia, Canada, through integration of compositional studies of lode and detrital gold with historical placer production: A template for evaluation of orogenic gold districts: Economic Geology, v. 111, p. 1321–1345.

Chapman, R.J., Leake, R.C., Moles, N.R., Earls, G., Cooper, C., Harrington, K., and Berzins, R., 2000a, The application of microchemical analysis of gold grains to the understanding of complex local and regional gold mineralization: a case study in Ireland and Scotland: Economic Geology, v. 95, p. 1753-1773.

Chapman, R.J., Leake, R.C., and Floyd, D.J., 2000b, Regional gold mineralization in the vicinity of the Glengaber Burn, Scottish Borders: Scottish Journal of Geology, v. 36, p. 165-176.

Chapman, R.J., Shaw, M.H., Leake, R.C., and Jackson, B., 2005, Gold in the central Ochil Hills, Scotland: Transactions of the Institution of Mining and Metallurgy (Section B Applied Earth Sciences), v. 114, p. 53-63.

Chapman, R.J. Leake, R.C., Bond, D.P.G., Stedra, V., and Fairgrieve, B., 2009, Chemical and mineralogical signatures of gold formed in oxidizing chloride hydrothermal systems and their significance within populations of placer gold grains collected during reconnaissance: Economic Geology, v. 104, 4**,** p. 563-585.

Chapman, R.J., Mortensen, J.K., Crawford, E. and LeBarge, W., 2010a, Microchemical studies of placer and lode gold in the Klondike District, Yukon, Canada: 1. Evidence for a small, gold-rich, orogenic hydrothermal system in the Bonanza and Eldorado Creek area: Economic Geology, v. 105, p. 1369–1392.

Chapman, R.J., Mortensen, J.K., Crawford, E.C., and LeBarge, W.P., 2010b, Microchemical studies of placer and lode gold in the Klondike District, Yukon, Canada: 2. Constraints on the nature and location of regional lode sources: Economic Geology, v. 105, p. 1393–1410.

Chapman, R., Mortensen, J., and LeBarge, W., 2011, Styles of lode gold mineralization contributing to the placers of the Indian River and Black Hills Creek, Yukon Territory, Canada as deduced from microchemical characterization of placer gold grains: Mineralium Deposita, v. 46, p. 881-903.

Chapman, R.J., Mileham, T., Allan, M.M. and Mortensen, J.K., 2017, A distinctive Pd-Hg signature in detrital gold derived from alkalic Cu-Au porphyry systems: Ore Geology Reviews, v. 83, p. 84-102.

Chapman, R.J., Allen, M.M., Mortensen, J.K., Wrighton, T.M. and Grimshaw, M.R., 2018, A new indicator mineral methodology based on a generic Bi-Pb-Te-S mineral inclusion signature in detrital gold from porphyry and epithermal environments in Yukon Territory, Canada: Mineralium Deposita, v. 53, p. 815-834.

Chapman, R.J., Banks, D.A, Styles, M.T, Walshaw, R.D., Piazolo, S., Morgan, D.J., Grimshaw, M.R., Spence-Jones, C.P., Matthews, T.J. and Borovinskaya, O., 2021, Chemical and physical heterogeneity within native gold: implications for the design of gold particle studies: Mineralium Deposita, https://doi.org/10.1007/s00126-020-01036-x

Craig, J.R., Solberg, T.N. and Linden, M.A., 1981, Compositional ranges of Appalachian gold: Society of Mining Engineers of AIME Transactions, v. 274, p. 1870-1872.

Crawford, E.C., 2007, Klondike placer gold: New tools for examining morphology, composition and crystallinity: Unpublished M.Sc. thesis, University of British Columbia, 151 p.

Desborough, G., Heidel, R., Raymond, W., and Tripp, J., 1971, Primary distribution of silver and copper in native gold from six deposits in the Western United States: Mineralium Deposita, v. 6, p. 321-334.

Dongmo, F.W., Chapman, R.J., Bolarinwa, A.T., Yongue, R.F., Banks, D.A. and Olajide-Kayode, J.O., 2019, Microchemical characterization of placer gold grains from the Meyos-Essabikoula area, Ntem complex, southern Cameroon: Journal of African Earth Sciences, v. 151, p. 189-201.

Fisher, N.H., 1945, The fineness of gold, with special reference to the Morobe gold field, New Guinea: Economic Geology, v. 40, p. 449-495.

Fuanya, C., Bolarinwa, A.T., Kankeu, B., Yongue, R.F., Ngatcha, R.B., and Tangko, T.E., 2019, Morphological and chemical assessment of alluvial gold grains from Ako'ozam and Njabilobe, southwestern Cameroon: Journal of African Earth Sciences. v. 154, p. 111-119.

Flower, K.A., 2018, MINFILE 092O 054: Ministry of Energy, Mines and Petroleum Resources, British Columbia Government. Gammons, C.H., and Williams-Jones, A.E., 1995, Hydrothermal geochemistry of electrum: Thermodynamic constraints: Economic Geology, v. 90, p. 420-432.

Godel, B., 2015, Platinum-group element deposits in layered intrusions: recent advances in the understanding of the ore forming processes: In Layered Intrusions (p. 379-432). Springer, Dordrecht.

Hart, C.J.R., 2007, Reduced intrusion-related gold systems, *in* Goodfellow, W.D., ed., Mineral deposits of Canada: A Synthesis of Major Deposit Types, District Metallogeny, the Evolution of Geological Provinces, and Exploration Methods: Geological Association of Canada, Mineral Deposits Division, Special Publication no. 5, p. 95-112.

Hashmi, S, Ward, B.C., Plouffe, A., Leybourne, M.I., and Ferbey, T., 2015, Geochemical and mineralogical dispersal in till from the Mount Polley Cu-Au porphyry deposit, central British Columbia; Canada; Geochemistry: Exploration, Environment, Analysis, v. 15, p. 234–249.

Henney, P.J., Styles, M.T., Bland, D.J. and Wetton, P.D., 1994, Characterization of gold from the Lubuk Mandi area, Terengganu, Malaysia: British Geological Survey, Technical Report WC/94/21.

Knight, J.B. and Leitch, C.H., 2001, Phase relations in the system Au–Cu–Ag at low temperatures, based on natural assemblages: The Canadian Mineralogist, v. 39, p. 889-905.

Knight, J.B., Mortensen, J.K. and Morison, S.R., 1999, Lode and placer gold composition in the Klondike District, Yukon Territory, Canada: Implications for the nature and genesis of Klondike placer and lode gold deposits: Economic Geology, v. 94, p. 649-664.

Lalomov, A.V., Chefranov, R.M., Naumov V.A., Naumova, O.B., LeBarge, W. and Dilly R.A., 2016, Typomorphic features of placer gold of Vagran cluster (the Northern Urals) and search indicators for primary bedrock gold deposits; Ore Geology Reviews, v. 85, p321-335

Leake, R.C., Bland, D.J., Styles, M.T. and Cameron, D.G., 1991, Internal structure of Au-Pd-Pt grains from South Devon, England, in relation to low temperature transport and deposition: Transactions of the Institution of Mining and Metallurgy (Section B Applied Earth Sciences), v. 100, p. B159-178.

Leake, R.C., Bland, D.J. and Cooper, C., 1992, Source characterization of alluvial gold from mineral inclusions and internal compositional variation: Transactions of the Institution of Mining and Metallurgy (Section B Applied Earth Sciences), v. 102, p. B65-82.

Leake, R.C., Chapman, R.J., Bland, D.J., Condliffe, E. and Styles, M.T., 1997, Microchemical characterization of gold from Scotland: Transactions of the Institution of Mining and Metallurgy (Section B Applied Earth Sciences), v. 106, p. B85-98.

Leake, R.C., Chapman, R.J., Bland, D.J., Stone, P., Cameron D.G. and Styles, M.T., 1998. The origin of alluvial gold in the Leadhills area of Scotland: evidence from internal chemical characteristics: Journal of Exploration Geochemistry, v. 63, p. 7-36.

Lefebure, D.V., 1996, Five-element veins Ag-Ni-Co-As+/-(Bi,U): *in* Selected British Columbia Mineral Deposit Profiles, Volume 2 - Metallic Deposits, Lefebure, D.V. and Hõy, T, Editors, British Columbia Ministry of Employment and Investment, Open File 1996-13, p. 89-92.

LeFort, D. Hanley, J and Guillong, M., 2011, Subepithermal Au-Pd Mineralization Associated with an Alkalic Porphyry Cu-Au Deposit, Mount Milligan, Quesnel Terrane, British Columbia, Canada: Economic Geology, v. 106, p. 781–808.

Liu, H., Beaudoin, G., Makvandi, S., Jackson, S.E. and Huang, X., 2021. Multivariate statistical analysis of trace element compositions of native gold from orogenic gold deposits: implication for mineral exploration: Ore Geology Reviews, v. 131, p. 104061.

Loen, J.S., 1995, Use of placer gold characteristics to locate bedrock gold mineralization: Exploration Mining Geology, v. 4, p. 335-339.

McClenaghan, M. B., and Cabri, L. J., 2011, Review of gold and platinum group element (PGE) indicator minerals methods for surficial sediment sampling: Geochemistry: Exploration, Environment, Analysis, v. 11, no. 4, p. 251-263.

McTaggart, K.C., and Knight, J., 1993, Geochemistry of lode and placer gold of the Cariboo District, BC: British Columbia Ministry of Energy, Mines and Petroleum Resources, Open File 1993-30, 25 p.

MacWilliam, K.R.G., 2018, The geology and genesis of the Coffee gold deposit in west-central Yukon, Canada: implications for the structural, magmatic, and metallogenic evolution of the Dawson Rage, and gold deposit models: Unpublished Thesis, University of British Columbia, 466p

Maloof, T.L., Baker T. and Thompson, J.F., 2001, The Dublin Gulch intrusion-hosted gold deposit, Tombstone plutonic suite, Yukon Territory, Canada: Mineralium Deposita. v. 36, p.583-593.

Marsh, E.E., Goldfarb, R.J., Hart, C.J.R. and Johnson, C.A., 2003, Geology and geochemistry of the Clear Creek intrusion-related gold occurrences, Tintina Gold Province, Yukon, Canada: Canadian Journal of Earth Sciences, v. 40, p. 681-699.

Mao, M., Rukhlov, A.S., Rowins, S.M., Spence, J. and Coogan, L.A., 2016, Apatite trace element compositions: A robust new tool for mineral exploration: Economic Geology, v. 111, p. 1187-1222.

Melchiorre, E.B. and Henderson, J., 2019, Topographic gradients and lode gold sourcing recorded by placer gold morphology, geochemistry, and mineral inclusions in the east fork San Gabriel River, California, USA: Ore Geology Reviews, v. 109, p. 348-357.

Moles, N.R. and Chapman, R.J., 2019, Integration of detrital gold microchemistry, heavy mineral distribution, and sediment geochemistry to clarify regional metallogeny in glaciated terrains: Application in the Caledonides of southeast Ireland: Economic Geology, v. 114, p. 207-232.

Morrison, G.W., Rose, W.J. and Jaireth, S., 1991, Geological and geochemical controls on the silver content (fineness) of gold in gold–silver deposits: Ore Geology Reviews, v. 6, p. 333-364.

Moeller, P. and Kersten, G., 1994, Electrochemical accumulation of visible gold on pyrite and arsenopyrite surfaces: Mineralium Deposita, v. 29, p. 404-413.

Naden, J., and Henney, P.J., 1995, Characterization of gold from Fiji: British Geological Survey, Technical Report WC/95/41.

Nevolko, P.A., Kolpakov, V.V., Nesterenko, G.G. and Fominykh, P.A., 2019, Alluvial placer gold of the Egor'evsk District (northern-western Salair): Composition characteristics, types and mineral microinclusions: Russian Geology and Geophysics, v. 60, p, 67-85.

Omang, B.O., Suh, C.E., Lehmann, B., Vishiti, A., Chombong, N.N., Fon, A.N, Egbe, J.A. and Shemang, E.M., 2015, Microchemical signature of alluvial gold from two contrasting terrains in Cameroon: Journal of African Earth Sciences, v. 112, p. 1-4.

Outridge, P.M., Doherty, W. and Gregoire, D.C., 1998, Determination of trace elemental signatures in placer gold by laser ablation–inductively coupled plasma–mass spectrometry as a potential aid for gold exploration: Journal of Geochemical Exploration, v. 60, p. 229-240.

Plouffe, A., and Ferbey, T., 2017, Porphyry Cu indicator minerals in till: A method to discover buried mineralization: *in* Ferbey, T., Plouffe, A., and Hickin, A.S., (Eds.), Indicator Minerals in Till and Stream Sediments of the Canadian Cordillera. Geological Association of Canada Special Paper Volume 50, and Mineralogical Association of Canada Topics in Mineral Sciences, v. 47, p. 129-159.

Petrella, L., Thébaud, N., Fougerouse, D., Evans, K., Quadir, Z. and Laflamme, C., 2020, Colloidal gold transport: a key to high-grade gold mineralization?: Mineralium Deposita, **v.** 55, p. 1247–1254.

Poulin, R.S., McDonald, A.M., Kontak, D.J., and McClenaghan, M.B., 2016, On the relationship between cathodoluminescence and the chemical composition of scheelite from geologically diverse ore deposit discriminator using its trace element and REE chemistry; The Canadian Mineralogist, v. 56, p. 265–302.

Poulin, R.S., McDonald, A.M., Kontak, D.J., and McClenaghan, M.B., 2018, Assessing scheelite ore deposit environments: The Canadian Mineralogist, v. 54, p. 1147–1173

Simon, G., Kesler, S.E., Essene, E.J. and Chryssoulis, S.L., 2000, Gold in porphyry copper deposits: experimental determination of the distribution of gold in the Cu–Fe–S system at 400 to 700 °C: Economic Geology, v.95, p. 259–270. https://doi.org/10.2113/gsecongeo.95.2.259

Staples, R.D., Gibson, H.D., Colpron, M. and Ryan, J.J., 2016, An orogenic wedge model for diachronous deformation, metamorphism, and exhumation in the hinterland of the northern Canadian Cordillera: Lithosphere, v. 8, p. 165-84.

Svetlitskaya, T.V.,, Nevolko P.A., Kolpakov,V.V., and Tolstykh, N.D., 2018, Native gold from the Inagli Pt–Au placer deposit (the Aldan Shield, Russia): geochemical characteristics and implications for possible bedrock sources: Mineralium Deposita, v. 53, p. 323-338.

Tarkian, M. and Stribrny, B., 1999, Platinum-group elements in porphyry copper deposits: A reconnaissance study: Mineralogy and Petrology, v. 65, p. 161-183.

Townley, B.K., Herail, G., Maksaev, V., Palacios, C., de Parseval, P., Sepuldeva, F., Orellana, R., Rivas, P., and Ulloa, C., 2003, Gold grain morphology and composition as an exploration tool: Application to gold exploration in covered areas: Geochemistry, Exploration, Environment, Analysis, v. 3, p. 29-38.

Wainwright, A. J., Simmons, A. T., Finnigan, C. S., Smith, T. R., and Carpenter, R. L., 2010, Geology of new gold discoveries in the Coffee Creek area, White Gold district, west-central Yukon: Yukon Exploration and Geology 2010, K.E. MacFarlane, L.H. Weston and C. Relf (Eds.), Yukon Geological Survey, p. 233-247.

Watling, R.J., Herbert, H.K., Delev, D., and Abell, I.D., 1994, Gold fingerprinting by laser-ablation inductively coupled plasma- mass spectrometry: Spectrochim Acta, v. 49B-2, p. 205-219.

Watling, R.J., Taylor, J.J., Shell, C.A., Chapman, R.J., Warner, R.B., Cahill, M., and Leake, R.C., 1999, The application of laser inductively-coupled mass spectrometry (LA-ICP-MS) for establishing the provenance of gold ores and artefacts. In: Young, M.M., Pollard, A.M., Budd, P., Ixer, R. (Eds.) Metals in Antiquity. BAR International Series 792, p. 142-154.

Wrighton, T.M., 2013, Placer gold microchemical characterization and shape analysis applied as an exploration tool in western Yukon: Unpublished MSc Thesis, University of British Columbia, 140 p.

Zaykov, V.V., Melekestseva I.Y., Zaykova, E.V, Kotlyarov, V.A. and Kraynev, Y.D., 2017, Gold and platinum group minerals in placers of the South Urals: Composition, microinclusions of ore minerals and primary sources: Ore Geology Reviews, v. 85, p.299-320.

Figure Captions

Figure 1. Study area and sample sites in western Canada.

Figure 2. Detail of gold sample localities in southern Yukon

Figure 3. Examples of opaque inclusions in Cordilleran gold particles. A: Gold-sphalerite association in lode sample comprising intergrowths and inclusions (Bralorne, B.C.); B: Galena inclusion in lode Au, Nugget Zone, Lone Star, Klondike, C: Pyrite inclusion in lode gold particle, Snowy Ck., Cassiar, BC; D: Pyrrhotite inclusion, detrital grain, Coffee Creek, Yukon; E: Galena and arsenopyrite inclusions detrital particle, Independence Creek, Yukon; F: Aguilarite (Ag_4SeS) inclusion in lode gold particle from Blackdome, B.C.;G; Inclusions of chalcocite in detrital gold particle from Bridge River, B.C., H: Mixed inclusion of Sb and Te-bearing galena and Bi telluride, Revenue Creek, Yukon, I: Arsenopyrite and galena, detrital grain, Soya Creek, Moosehorn Range, Yukon

Figure 4. Evaluation of approaches to characterizing five sample sets, chosen to represent different deposit types: Orogenic, (Wells '2', BC, data from Chapman and Mortensen, 2016), Epizonal orogenic (Thistle Creek and environs, Yukon, data from Wrighton, 2013), Intermediate sulfidation (Klaza, Yukon, data from Chapman et al; 2018), calc-alkalic Cu-Au-Mo porphyry (Nucleus Revenue, Yukon, data from Chapman et al. 2018), alkalic Cu-Au porphyry (Similkameen River and tributaries, BC, data from Chapman et al., 2017). Mineral abbreviations in Fig. 4C: Py = pyrite, Po = pyrrhotite, Gn = galena, Cpy = chalcopyrite, Sph = sphalerite, Bn = bornite, CC = chalcocite, Mo = molybdenite, Apy = arsenopyrite, Grs = gersdorffite, cob= cobaltite, Lo= loellingite, Ac = acanthite, Pet = petzite, Cv = cervelleite, Hs = hessite, Bi= native bismuth, Tet= tetrahedrite, Ul = ullmanite, Tem = temagamite. All symbols comprising chemical symbols denote undifferentiated minerals of that composition.

Figure 5. Workflow for construction of radar diagrams to represent the elemental composition of inclusions within a population of gold particles. .

Figure 6. Inclusion signatures of ~~populations~~ gold from lode and placer sample populations for orogenic systems showing the S-As±Sb non-metal signature. Lode samples are indicated by solid text headings. Metal signatures are similar throughout.

Fig 7. Inclusion signatures of gold in sample populations from orogenic gold districts which contain the Ag-Te association. Lode samples are indicated by solid text headings.

Figure 8. Inclusion signatures of gold formed in magmatic-hydrothermal systems. Lode samples are indicated by solid text headings.

Figure 9. Comparison of inclusion signatures of gold from the North American Cordillera and other localities worldwide. Lode samples are indicated by solid text headings.

Table 1a Sample sets from previous work used in this study

Sample set name	Locality/ Region/Country	Component samples	Placer/ Hypogene	No. Particles	No. Inclusions	Reference
		Orogenic Gold Mineralization				
Wells 1	Cariboo Gold District, BC, Canada	Cow Mtn lode, Lowhee, Burns, Chisholm Creeks	P+H	370	54	Chapman and Mortensen (2016)
Wells 2	Cariboo Gold District, BC, Canada	Warspite, Myrtle lodes. Cunningham, Antler, Williams, Keithley, Little Snowshoe, Maude, creeks	P+H	611	34	Chapman and Mortensen (2016)
Nugget/Buckland Zone	Lone Star, Klondike, Yukon, Canada	Buckland and Nugget zone samples 1-4	H	553	48	Chapman et al. 2010a
Boulder Lode	Lone Star, Klondike, Yukon, Canada	Lone Star 1-5	H	359	47	Chapman et al. 2010a
Hunker Dome	Klondike, Yukon, Canada	Mitchell vein, Hunker Dome lode, Sheba East lode	H	600	105	Chapman et al. 2010b
Sixtymile District	Yukon, Canada	Glacier, Miller Creeks	P	154	10	Wrighton, (2013)
Indian River	Yukon, Canada	IR1-5, Lower Quartz, Lower Dominion creeks	P	1420	77	Chapman et al. (2011)
Tenmile Ck	Yukon, Canada	Main channel, 2 tributaries	P	353	79	Wrighton, (2013)
Last Chance Ck	Klondike, Yukon, Canada	Lindow, Bear, Last Chance creeks	P	425	70	Chapman et al. 2010b
Mackinnon Ck	White Gold District, Yukon, Canada		H	76	35	Wrighton, (2013)
Thistle Creek	Yukon, Canada	Upper and mid Thistle, Blueberry, Lulu, Kirkman, Barker, creeks, Pete's Gulch	P	481	158	Wrighton, (2013)
Maisy May Ck	Yukon, Canada	Upper Maisy May and tributary.	P	182	27	Wrighton, (2013)
Scroggie Ck	Yukon, Canada		P	100	37	Wrighton, (2013)
Eureka Ck and environs	Yukon, Canada	Eureka, Montana, Stowe, Diversion, Blackhills 1-3 creeks	P	604	161	Chapman et al. (2011)
Lone Star type 1d	Lone Star, Klondike, Yukon, Canada	Skookum, Adams, Little Blanche, Canyon creeks	P	494	45	Chapman et al. 2010a
Lone star type 1f	Lone Star, Klondike, Yukon, Canada	Eldorado 3,4, Gay Gulch (lower) 7 Pup, Melissa creeks	P	696	108	Chapman et al. 2010a
Upper Henderson Ck	Yukon, Canada		P	61	8	Wrighton, (2013)
Mid Henderson Ck	Yukon, Canada		P	415	47	Wrighton, (2013)
N Henderson Ck	Yukon, Canada	North Henderson , Moosehorn creeks	P	395	71	Wrighton, (2013)
		Magmatic Hydrothermal Mineralization				
Revenue/Nucleus	Yukon, Canada	Revenue and Mechanic Creeks	P	654	156	Chapman et al. (2018)
Casino, porphyry	Yukon, Canada	As defined by Chapman et al. (2018)	P+H	122	27	Chapman et al. (2018)

Canadian Ck	Yukon, Canada	As defined by Chapman et al.(2018)	P+H	84	24	Chapman et al. (2016, 2018)
Klaza	Yukon, Canada	Nansen, Canaan, Victoria creeks, BRX eluvial	P+H	585	41	Chapman et al. (2017)
Similkameen R	S BC, Canada		P	244	68	Chapman et al. (2017)
Cherry Ck	S Central BC, Canada		P	59	10	Chapman et al. (2017)

Table 1b. Sample sets not previously reported used in this study

Sample set name	Locality/ Region/Country	Placer/ Hypogene	Sample origin/ descriptions	No. Particles	No. Inclusions
Bralorne	S. BC, Canada	P+H	UBC collections	112	18
Cassiar	N BC, Canada	P+H	UBC collections	344	60
Coffee Environs	Yukon, Canada	P	Independence, Shovel creeks, Yukon	206	84
Black Dome	BC, Canada	H	UBC collections	501	150
Moosehorn Range	SW Yukon, Canada	P	Mine R., Swamp, Soya, MacArthur creeks	479	50
Dublin Gulch	Yukon, Canada	P	Donated sample (J. Bond, YGS)	116	25
Clear Ck	Yukon, Canada	P	Donated sample W. LeBarge, (YGS)	149	35
Atlin District	Northern BC, Canada	P	Donated samples: Otter, Ruby, Quartz, Wright, Feather, Pine, Boulder creeks	487	58
Stirrup Ck	BC. Canada	P	UBC collections	259	52
Siwash Ck	BC, Canada	P	UBC collections	87	26
Wheaton Ck	BC, Canada	P	UBC collections	109	34
Friday Ck	S BC, Canada	P	Additional data to that reported in Chapman et al. (2017)	173	34
KSM drainage	BC, Canada	P	Mitchell and Sulphurettes creeks	443	41

Table 1c. Sample sets from other studies worldwide used in this study.

Locality	Contributing samples	Style of Mineralization	No. Particles	No. Inclusions	Reference
Leadhills type 1	Shortcleugh Water	Orogenic	500	85	Leake et al. (1997)
Southern Uplands, Sotland	Glengaber Burn and environs, R. Tweed	Orogenic	811	144	Chapman et al. (2000 b)
Wexford, Ireland	Sample sites described by Moles and Chapman (2019)	Orogenic	1428	139	Moles and Chapman (2019)
Co. Mayo, Ireland	Carrownisky R., Bunowen R. Croagh Patrick (hypogene and placer), Srahrooskey (hypogene).	Orogenic	295	58	Chapman et al. (2000a)
Malaysia	Lubuk Mandi	Orogenic	207	72	Henney et al. (1994)
Ochil Hills, Scotland	Gold type 1 identified by Chapman et al. (2005)	Epithermal	1059	74	Chapman et al. (2005)
Ochil Hills, Scotland	Gold type 2, phases 1 and 2 identified by Chapman et al. (2005),	Epithermal	127	68	Chapman et al. (2005)
Wainmanu R. Fiji	Epithermal gold type identified in Naden and Henney (1995)	Epithermal	46	13	Naden and Henney (1995)

Table 2. Stages in characterizing inclusion suites using radar diagrams and justification for methodology adopted.

Methodology	Justification
1. For minerals containing a metal and non-metal the metal score is 1 and the non metal score is 1.	
2. For minerals containing multiple elements the main components are scored equally, irrespective of stoichiometry: e.g., the score for chalcopyrite ($CuFeS_2$) is the same score as for bornite (Cu_5FeS_4): i.e., Cu=Fe= 0.5, S=1	Adoption of a scoring-based approach based on stoichiometric formulae would generate biases according to the formula concerned: e.g., covellite (CuS) would return Cu=1, S=1 whereas digenite would return Cu=9, S=10. Additionally the data base available to this study do not include stoichiometry for mineral inclusions where this cannot be gleaned from EDS spectra. Generation of a complete data set describing the accurate stoichiometry of inclusions in over 35,000 gold particles in historic data sets is not a realistic proposition.
3. Where substitution has been identified by a small EDS trace, the element is assigned a concentration of 0.1, with other elements being reduced pro rata	This approach acknowledges the presence of minor elements which are otherwise difficult to assimilate. The cumulative effect of several inclusions which contain substituted elements enhances the potential of the resulting diagram to discriminate between sample populations
4. Where inclusions are 'mixed' (e.g., Fig. 3 H, I) they are treated as separate inclusions	
5. Metal scores and non-metal scores are summed to provide totals for each element	The 'number of inclusions' sum = the number of particles in which a specific inclusion occurs. The number of inclusions of the same mineral within an individual gold particle does not affect the score.
6. For each category, each element is expressed as a percentage of the combined element score	
7. Datasets are depicted on pairs of radar diagrams describing metallic and non-metallic signatures using a log scale.	Many inclusion suites are dominated by common and non-diagnostic minerals such as pyrite, whereas the characterization of the assemblage may depend on other less abundant inclusions. These signatures are more clearly depicted using a log scale.

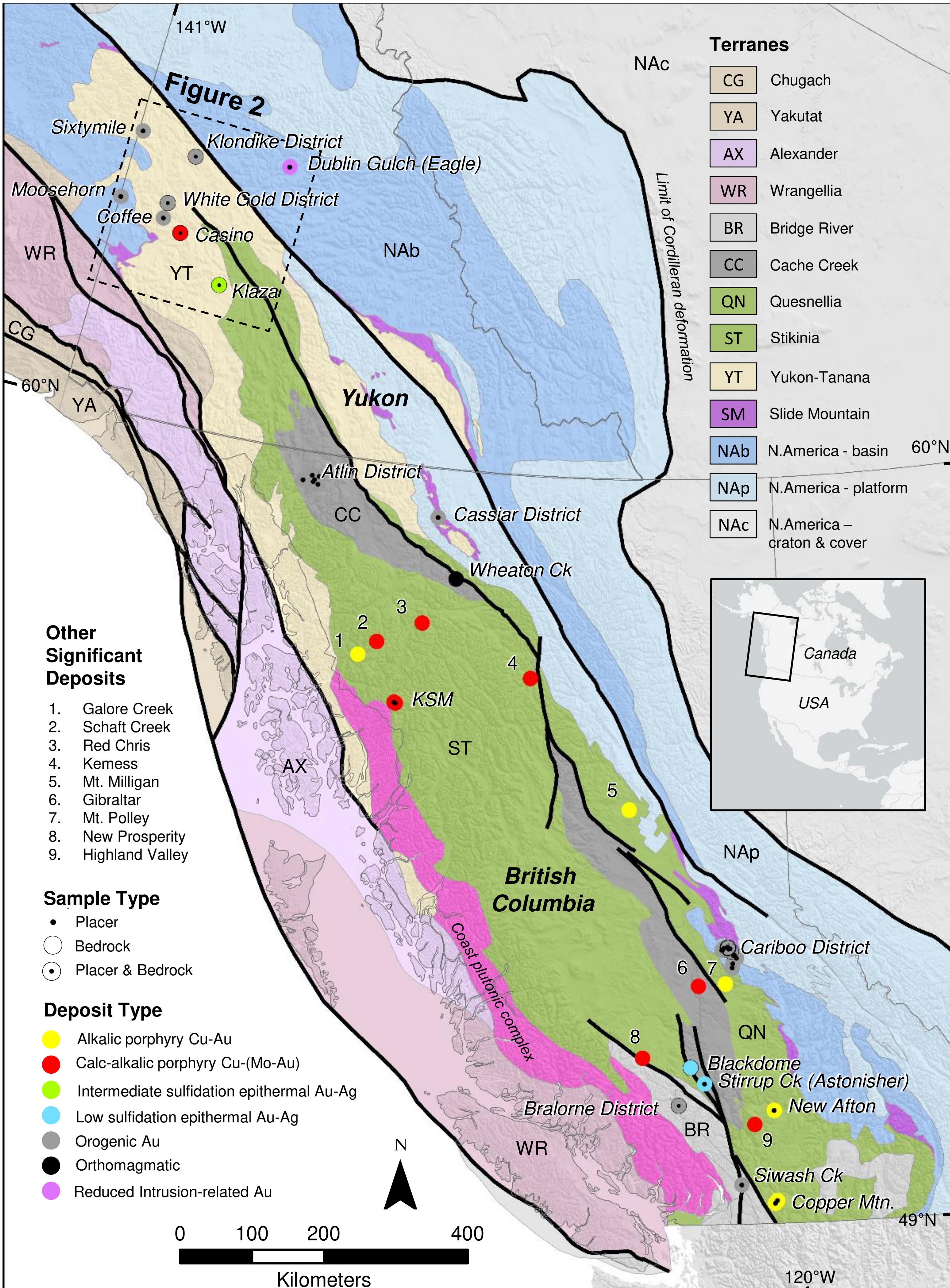

141°W
Figure 2
Sixtymile
Klondike District
Dublin Gulch (Eagle)
Moosehorn
White Gold District
Coffee
Casino
WR
YT
Klaza
NAb
NAc
CG
60°N
YA
Yukon
Atlin District
CC
Cassiar District
Wheaton Ck
Limit of Cordilleran deformation
Terranes
CG Chugach
YA Yakutat
AX Alexander
WR Wrangellia
BR Bridge River
CC Cache Creek
QN Quesnellia
ST Stikinia
YT Yukon-Tanana
SM Slide Mountain
NAb N.America - basin
NAp N.America - platform
NAc N.America – craton & cover
60°N
Canada
USA
1
2
3
4
KSM
ST
AX
5
NAp
British Columbia
Coast plutonic complex
Cariboo District
6
7
QN
8
Blackdome
Stirrup Ck (Astonisher)
New Afton
Bralorne District
BR
9
WR
Siwash Ck
Copper Mtn.
49°N
120°W
Other Significant Deposits
1. Galore Creek
2. Schaft Creek
3. Red Chris
4. Kemess
5. Mt. Milligan
6. Gibraltar
7. Mt. Polley
8. New Prosperity
9. Highland Valley
Sample Type
Placer
Bedrock
Placer & Bedrock
Deposit Type
Alkalic porphyry Cu-Au
Calc-alkalic porphyry Cu-(Mo-Au)
Intermediate sulfidation epithermal Au-Ag
Low sulfidation epithermal Au-Ag
Orogenic Au
Orthomagmatic
Reduced Intrusion-related Au
N
0 100 200 400
Kilometers

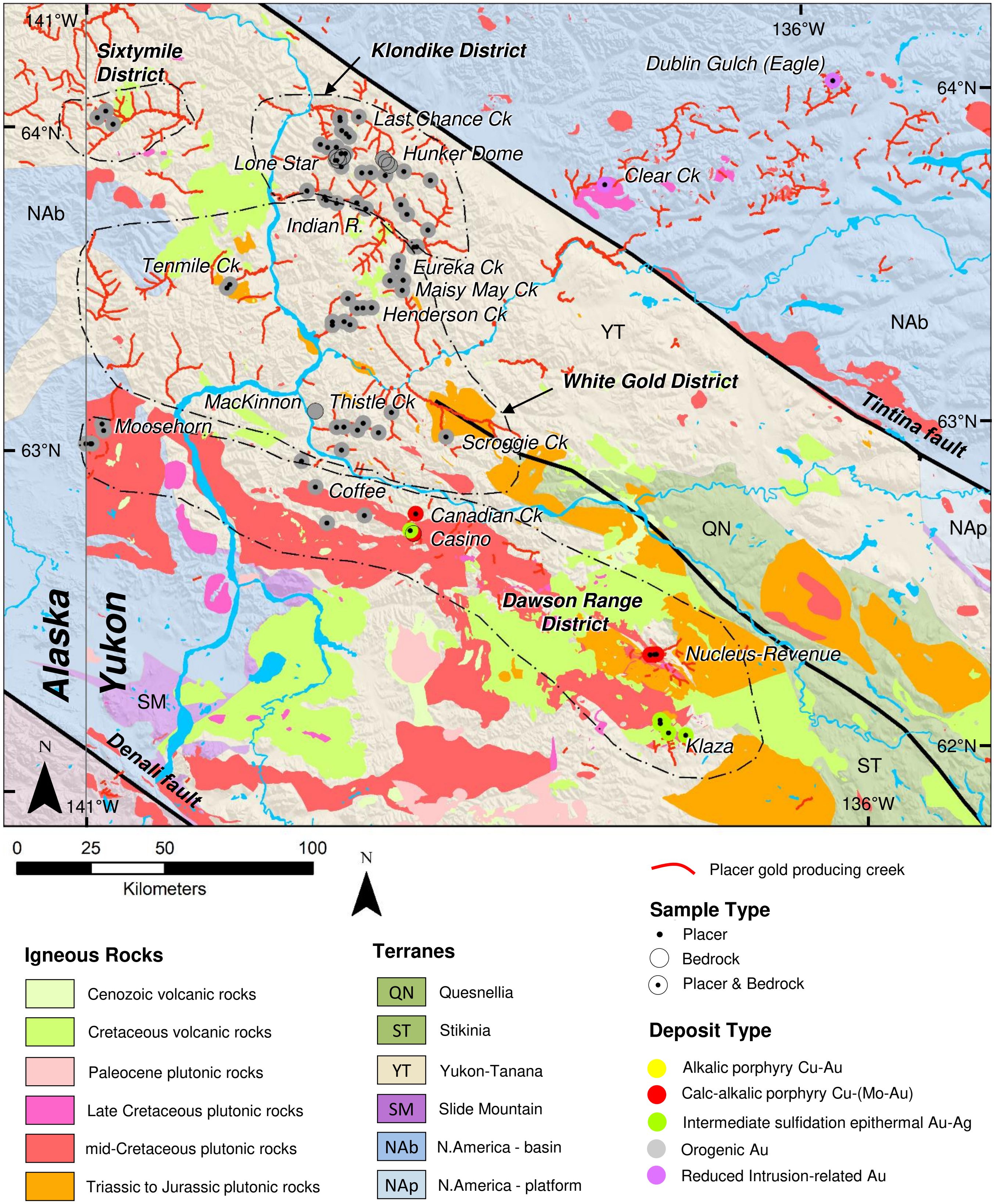

141°W
Sixtymile District
Klondike District
136°W
Dublin Gulch (Eagle)
64°N
Last Chance Ck
Lone Star
Hunker Dome
Clear Ck
NAb
Indian R.
Tenmile Ck
Eureka Ck
Maisy May Ck
Henderson Ck
YT
NAb
White Gold District
MacKinnon
Thistle Ck
Tintina fault
63°N
Moosehorn
Scroggie Ck
Coffee
Canadian Ck
Casino
QN
NAp
Dawson Range District
Nucleus-Revenue
Alaska
Yukon
SM
Klaza
62°N
ST
N
Denali fault
141°W
136°W
0
25
50
100
Kilometers
N
Placer gold producing creek
Sample Type
Placer
Bedrock
Placer & Bedrock
Igneous Rocks
Cenozoic volcanic rocks
Cretaceous volcanic rocks
Paleocene plutonic rocks
Late Cretaceous plutonic rocks
mid-Cretaceous plutonic rocks
Triassic to Jurassic plutonic rocks
Terranes
QN Quesnellia
ST Stikinia
YT Yukon-Tanana
SM Slide Mountain
NAb N.America - basin
NAp N.America - platform
Deposit Type
Alkalic porphyry Cu-Au
Calc-alkalic porphyry Cu-(Mo-Au)
Intermediate sulfidation epithermal Au-Ag
Orogenic Au
Reduced Intrusion-related Au

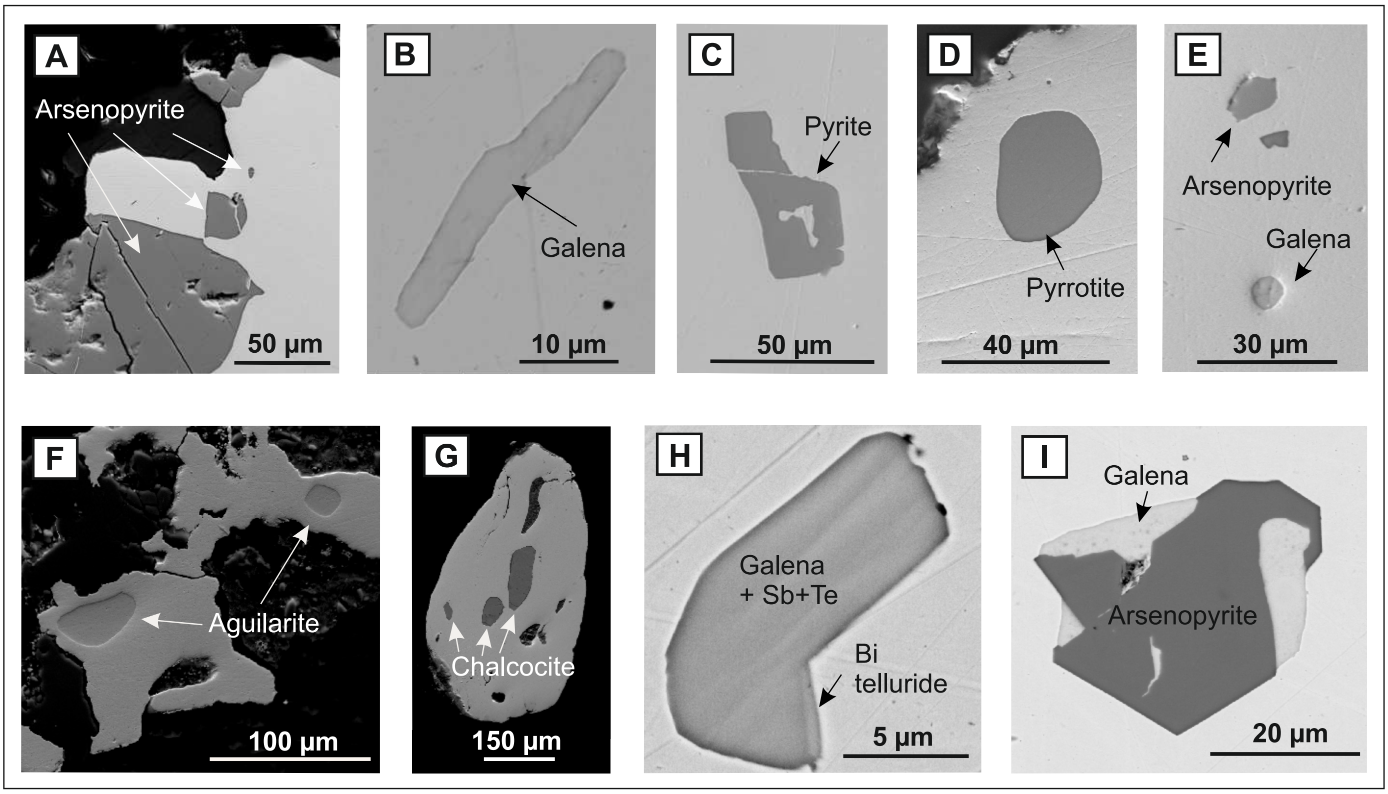
A
Arsenopyrite
50 µm
B
Galena
10 µm
C
Pyrite
50 µm
D
Pyrrotite
40 µm
E
Arsenopyrite
Galena
30 µm
F
Aguilarite
100 µm
G
Chalcocite
150 µm
H
Galena
+ Sb+Te
Bi
telluride
5 µm
I
Galena
Arsenopyrite
20 µm

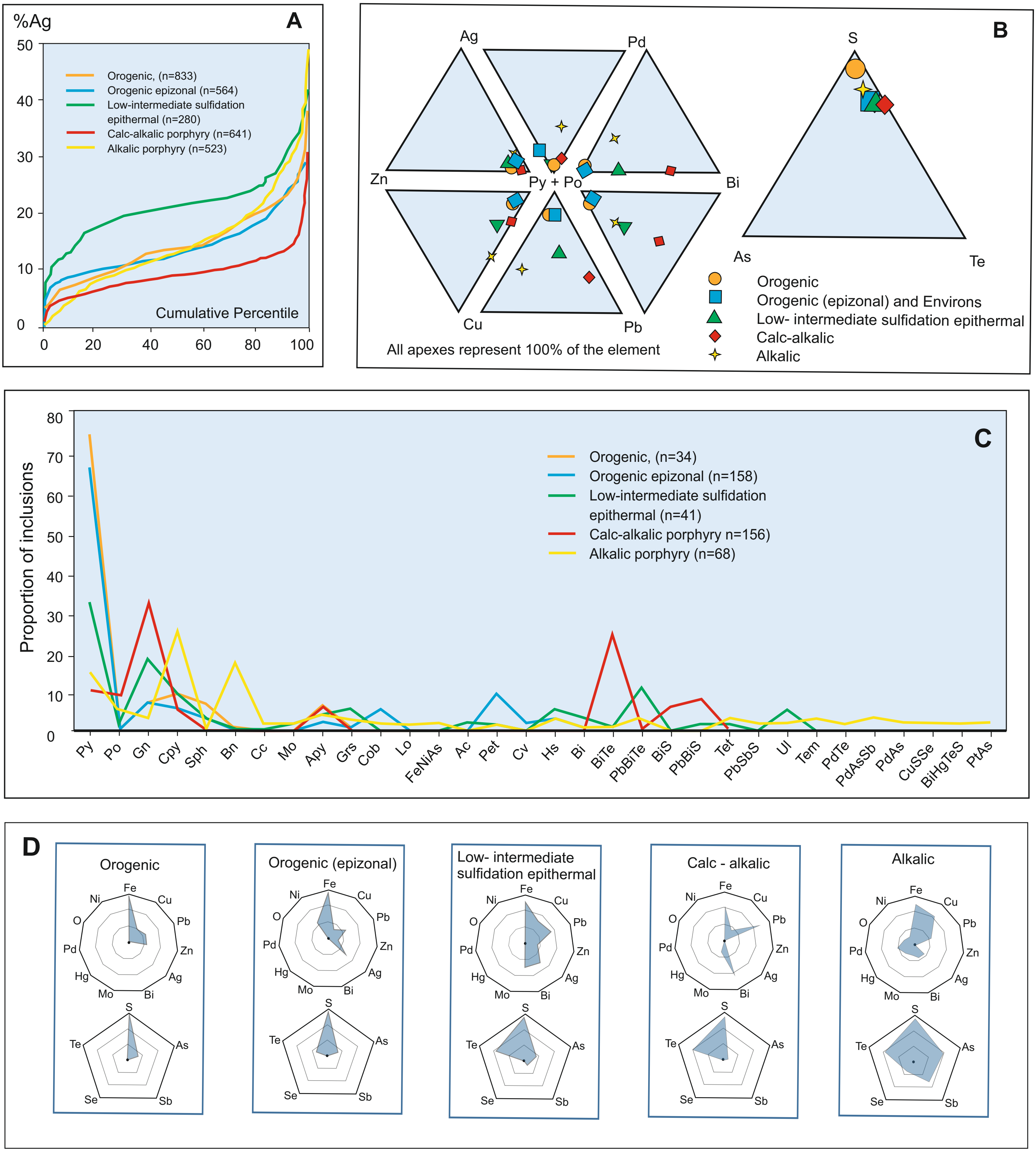

A
%Ag
Orogenic, (n=833)
Orogenic epizonal (n=564)
Low-intermediate sulfidation epithermal (n=280)
Calc-alkalic porphyry (n=641)
Alkalic porphyry (n=523)
Cumulative Percentile
B
Ag
Pd
Zn
Py + Po
Bi
Cu
Pb
S
As
Te
All apexes represent 100% of the element
Orogenic
Orogenic (epizonal) and Environs
Low- intermediate sulfidation epithermal
Calc-alkalic
Alkalic
C
Proportion of inclusions
Orogenic, (n=34)
Orogenic epizonal (n=158)
Low-intermediate sulfidation epithermal (n=41)
Calc-alkalic porphyry n=156)
Alkalic porphyry (n=68)
Py Po Gn Cpy Sph Bn Cc Mo Apy Grs Cob Lo FeNiAs Ac Pet Cv Hs Bi BiTe PbBiTe BiS PbBiS Tet PbSbS Ul Tem PdTe PdAsSb PdAs CuSSe BiHgTeS PtAs
D
Orogenic
Orogenic (epizonal)
Low- intermediate sulfidation epithermal
Calc - alkalic
Alkalic
Fe Cu Pb Zn Ag Bi Mo Hg Pd O Ni
S As Sb Se Te

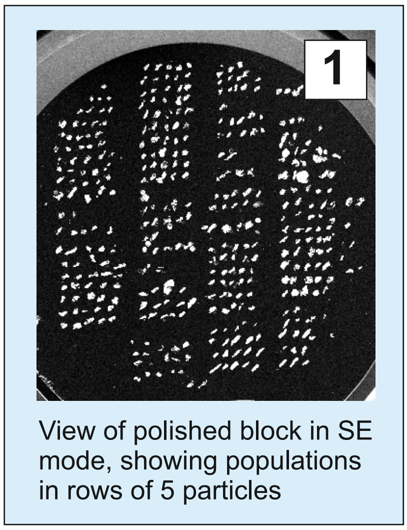

2

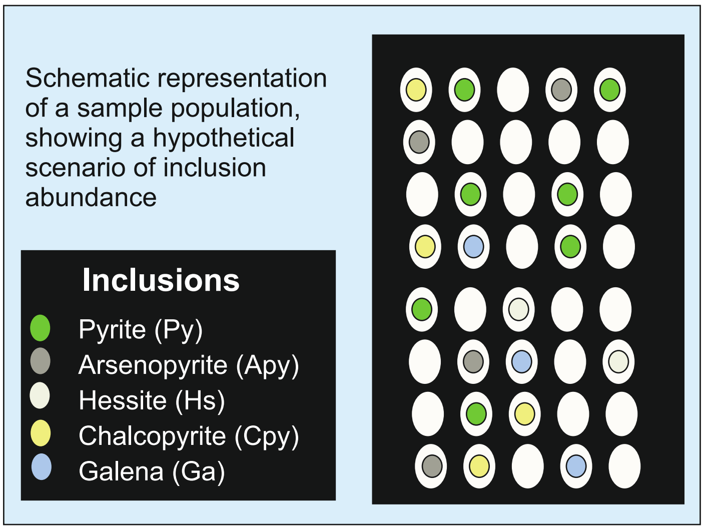

Number of particles containing an inclusion species are tallied and component elements scored

3

		Inclusion	Py	Apy	Hs	Cpy	Ga	Total	% of Total
		Number	7	4	2	4	3	20	100
		Element							
SCORING	Metals	Fe	7	4		2		13	65
		Cu				2		2	10
		Pb					3	3	15
		Ag			2			2	10
	Non metals	S	7	2		4	3	16	80
		As		2				2	10
		Te			2			2	10

4

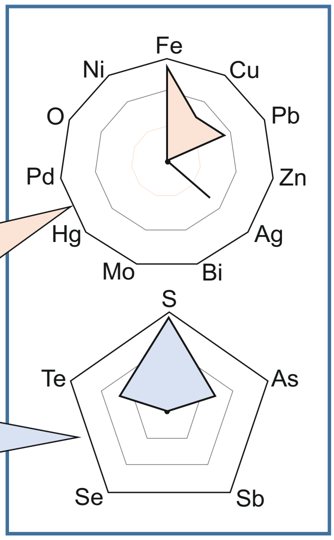

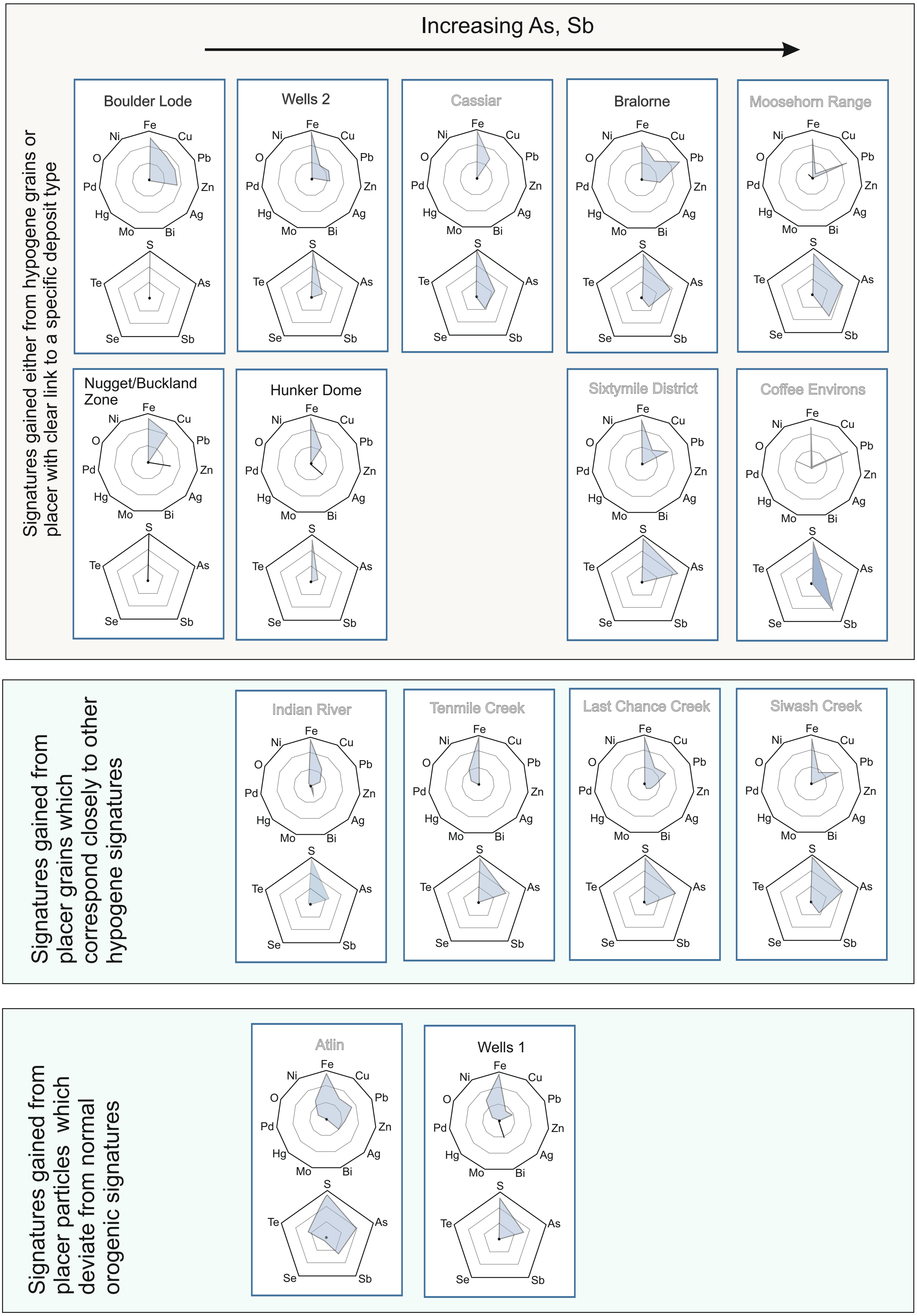
Increasing As, Sb
Signatures gained either from hypogene grains or placer with clear link to a specific deposit type
Boulder Lode
Wells 2
Cassiar
Bralorne
Moosehorn Range
Nugget/Buckland Zone
Hunker Dome
Sixtymile District
Coffee Environs
Signatures gained from placer grains which correspond closely to other hypogene signatures
Indian River
Tenmile Creek
Last Chance Creek
Siwash Creek
Signatures gained from placer particles which deviate from normal orogenic signatures
Atlin
Wells 1
Fe
Cu
Pb
Zn
Ag
Bi
Mo
Hg
Pd
O
Ni
S
As
Sb
Se
Te

Epizonal

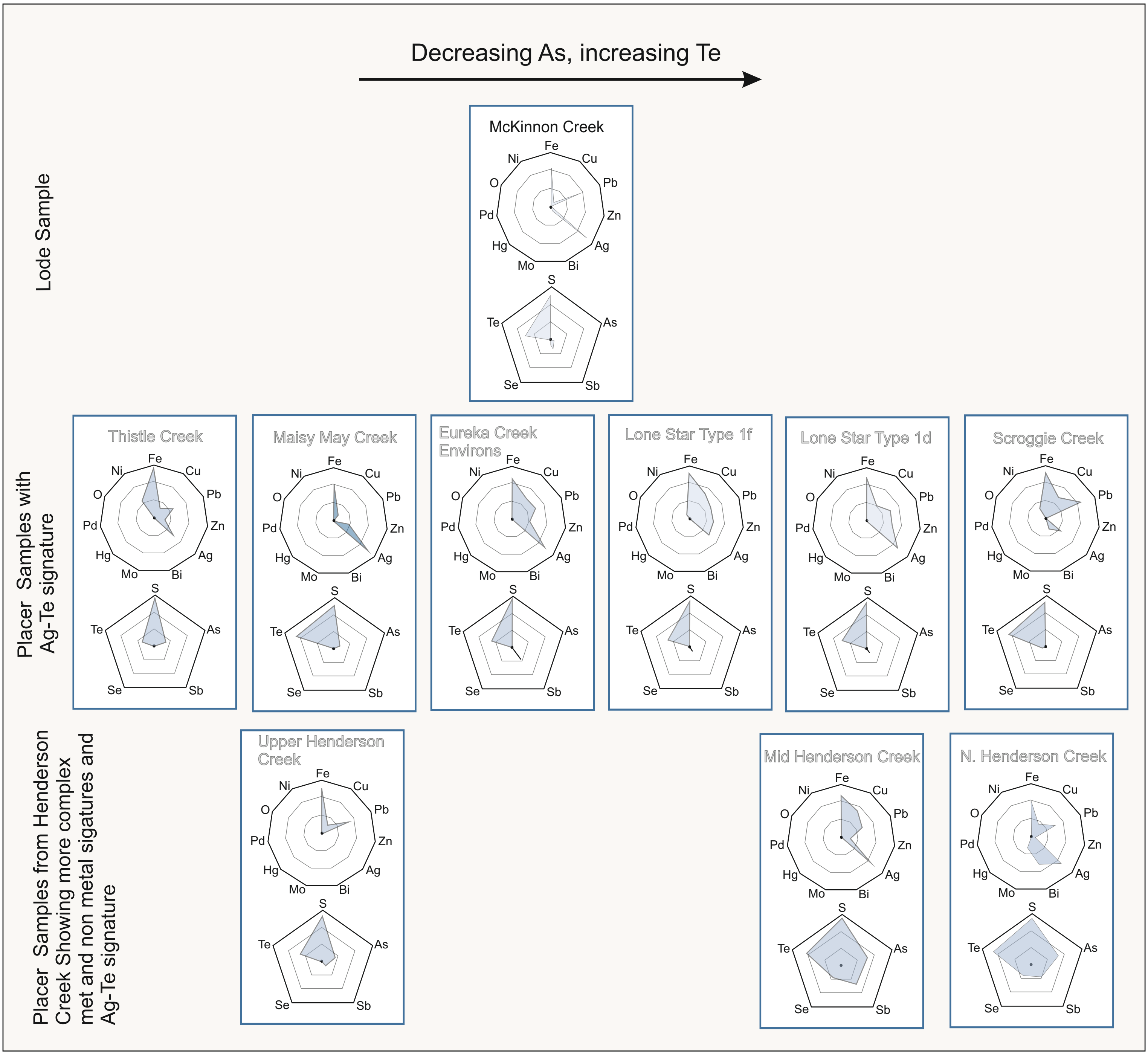
Decreasing As, increasing Te
Lode Sample
McKinnon Creek
Placer Samples with Ag-Te signature
Thistle Creek
Maisy May Creek
Eureka Creek Environs
Lone Star Type 1f
Lone Star Type 1d
Scroggie Creek
Placer Samples from Henderson Creek Showing more complex met and non metal sigatures and Ag-Te signature
Upper Henderson Creek
Mid Henderson Creek
N. Henderson Creek
Fe
Cu
Pb
Zn
Ag
Bi
Mo
Hg
Pd
O
Ni
S
As
Sb
Se
Te

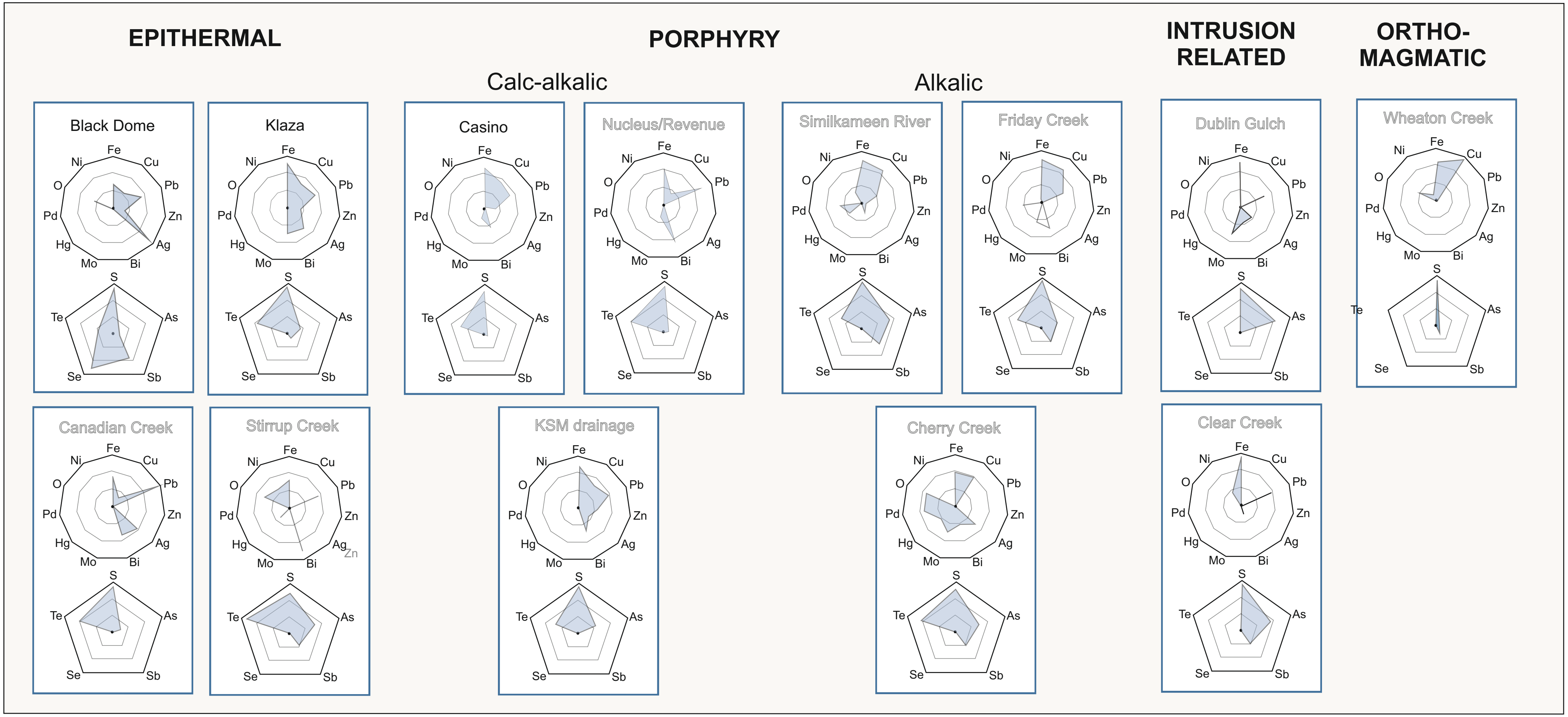
EPITHERMAL
PORPHYRY
Calc-alkalic
Alkalic
INTRUSION RELATED
ORTHO-MAGMATIC
Black Dome
Klaza
Casino
Nucleus/Revenue
Similkameen River
Friday Creek
Dublin Gulch
Wheaton Creek
Canadian Creek
Stirrup Creek
KSM drainage
Cherry Creek
Clear Creek
Fe
Cu
Pb
Zn
Ag
Bi
Mo
Hg
Pd
O
Ni
S
As
Sb
Se
Te

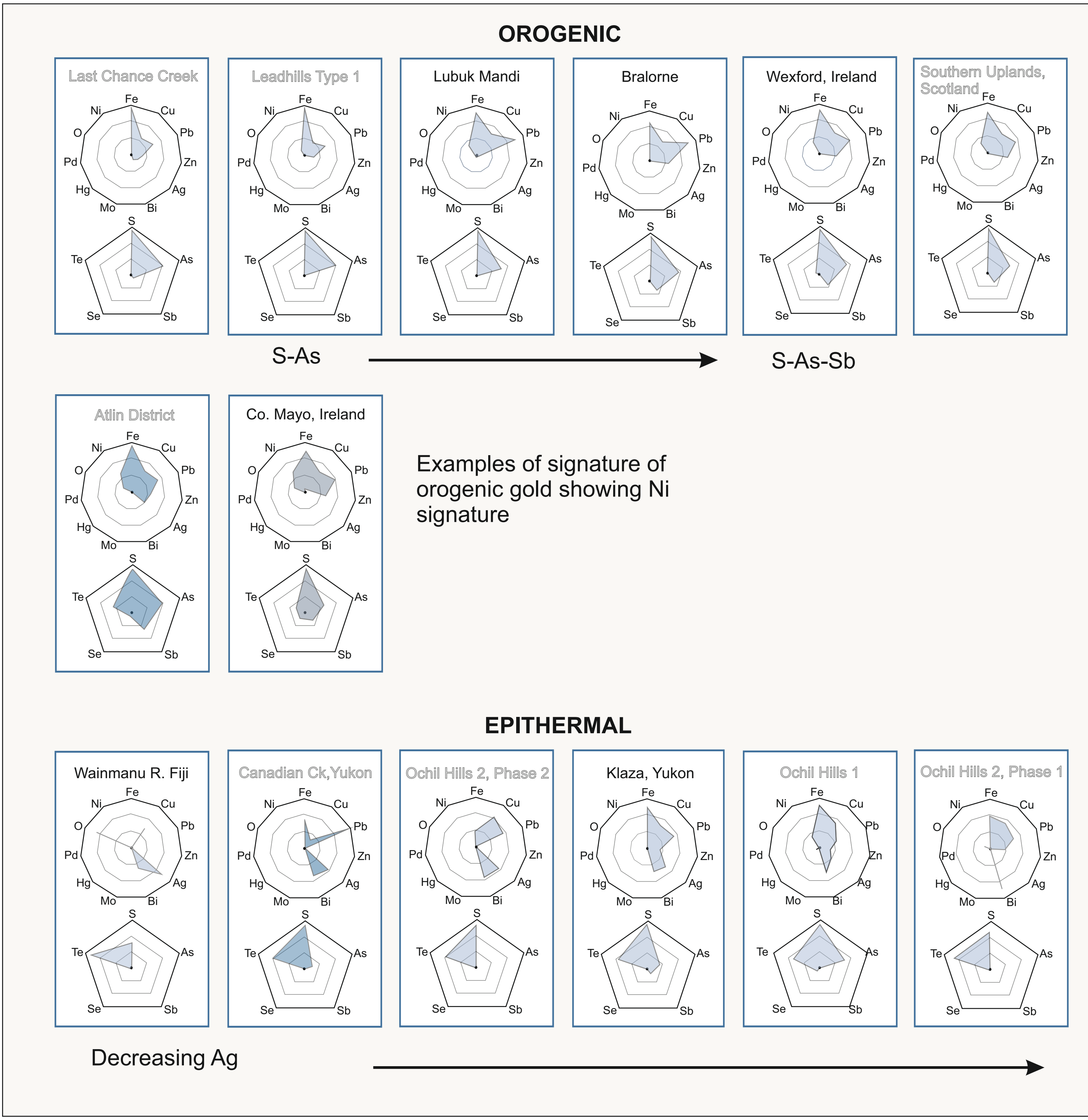
OROGENIC
Last Chance Creek
Leadhills Type 1
Lubuk Mandi
Bralorne
Wexford, Ireland
Southern Uplands, Scotland
S-As
S-As-Sb
Atlin District
Co. Mayo, Ireland
Examples of signature of orogenic gold showing Ni signature
EPITHERMAL
Wainmanu R. Fiji
Canadian Ck,Yukon
Ochil Hills 2, Phase 2
Klaza, Yukon
Ochil Hills 1
Ochil Hills 2, Phase 1
Decreasing Ag